Biomaterials Science

ROYAL SOCIETY OF CHEMISTRY

REVIEW

View Article Online
View Journal | View Issue

Cite this: *Biomater. Sci.*, 2023, **11**, 5390

Recent progress in PLGA-based microneedle-mediated transdermal drug and vaccine delivery

Atefeh Malek-Khatabi,[a] Malihe Sadat Razavi,[c,e] Alyeh Abdollahi,[a] Milad Rahimzadeghan,[d] Fatemeh Moammeri,[g] Mojgan Sheikhi,[f] Mohamadreza Tavakoli,[e] Mazda Rad-Malekshahi*[a] and Zahra Faraji Rad *[b]

Microneedles (MNs) have recently been found to have applications in drug, vitamin, protein and vaccine delivery. Polymeric MN arrays continue to attract increasing attention due to their capability to bypass the skin's stratum corneum (SC) barrier with minimal invasiveness. These carriers can achieve the targeted intradermal delivery of drugs and vaccines and improve their transdermal delivery level. As a nontoxic FDA-approved copolymer, polylactic glycolic acid (PLGA) has good biocompatibility and biodegradability. Currently, PLGA-based MNs have a noticeable tendency to be utilized as a delivery system. This study focuses on the most recent advances in PLGA-based MNs. Both PLGA nanoparticle-based MNs and PLGA matrix-based MNs, created for the delivery of vaccines, drugs, proteins and other therapeutic agents, are discussed. The paper also discusses the various types of MNs and their potential applications. Finally, the prospects and challenges of PLGA-based MNs are reviewed.

Received 9th May 2023,
Accepted 7th June 2023

DOI: 10.1039/d3bm00795b

rsc.li/biomaterials-science

1. Introduction

1.1. Microneedles

In recent decades, MN usage has grown beyond its traditional medicinal applications to include long-term disease therapy, immunobiological delivery, disease detection, and cosmetics.[1,2] In addition to small molecule drugs, MNs can be applied to transport abundant macromolecules, including proteins, growth hormones, receptor agonists, immunobiological vaccines and peptides, in a controlled way.[4,5] MNs can successfully bypass the SC, the main barrier to transdermal drug delivery, and transport their therapeutic payloads into the deeper layer of skin to increase drug efficacy for the long-term treatment of diseases and for immunobiological administration.[1,3] MNs are classified into five types based on the various drug delivery mechanisms (Fig. 1).[4–6] They are categorized as solid MNs, which are used for skin pre-treatment; coated MNs, which contain water-soluble pharmaceutical systems coated on the surface; dissolving MNs, which leave no remaining fragments; hollow MNs, which are used to transport a liquid formula through channels; and hydrogel-forming MNs.[4,7]

1.1.1. Solid MNs. Solid MNs can be designed for skin pre-treatment to deliver medications through pores. Topical systems (including ointments, gels and lotions) can be transported into the dermis through the micropores created on the skin.[8] This enables topical systems to be dispersed to body parts *via* the systemic circulation.[9]

1.1.2. Hollow MNs. Hollow MNs, unlike the others, are not restricted to low dosages and thus do not weaken therapeutic impact. Furthermore, the ability of hollow MNs to transport a wide range of chemicals and extract tissue fluids has attracted much interest.[8,10] However, they are prone to fracture due to a lack of tensile stability and are more challenging to manufacture.[7]

1.1.3. Coated MNs. Coated MNs can deliver therapeutic agents loaded onto the surface of the MNs and improve the penetration of the encapsulated agent. Negatively charged drugs, DNA or viruses are easily absorbed onto positively charged MNs, resulting in the MN coating. However, the maximum dosage of the drug is low.[3] Coated MNs have been used to deliver small molecules, macromolecules, vaccines, DNA and nanoparticles.[7]

1.1.4. Hydrogel-forming MNs. Hydrogel-forming MNs (HFMs) are made from crosslinked polymers that are hydro-

[a]*Department of Pharmaceutical Biomaterials and Medical Biomaterials Research Center, Faculty of Pharmacy, Tehran University of Medical Sciences, Tehran, Iran*
[b]*School of Engineering, University of Southern Queensland, Springfield, QLD 4300, Australia. E-mail: zahra.farajirad@usq.edu.au*
[c]*Department of Pharmaceutics, Faculty of Pharmacy, Mazandaran University of Medical Sciences, Sari, Iran*
[d]*Functional Neurosurgery Research Center, Shohada Tajrish Comprehensive Neurosurgical Center of Excellence, Shahid Beheshti University of Medical Sciences, Tehran, Iran*
[e]*Nanotechnology Research Centre, Faculty of Pharmacy, Tehran University of Medical Sciences, Tehran, Iran*
[f]*Department of Drug and Food Control, Faculty of Pharmacy, Tehran University of Medical Sciences, Tehran, Iran*
[g]*Department of Laboratory Sciences, School of Paramedical Sciences, Mashhad University of Medical Sciences, Mashhad, Iran*

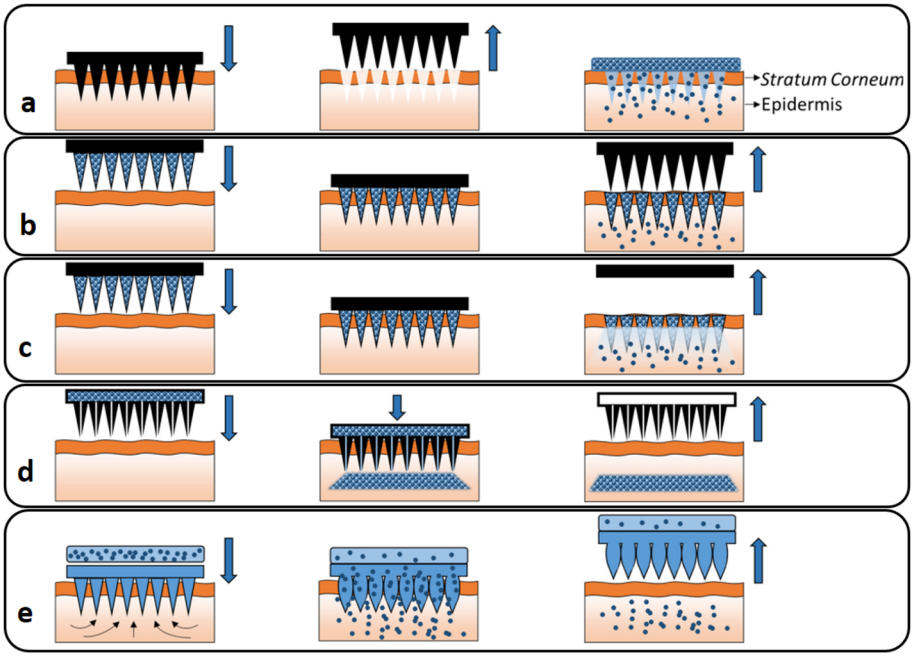

Fig. 1 Different types of MNs: (a) solid, (b) coated, (c) dissolving, (d) hollow and (e) hydrogel-forming MNs. Reproduced from ref. 10 with permission from Elsevier, copyright 2016.

philic and swellable. Because of the polymer's intrinsic hydrophilicity, the hydrogel MN swells upon application to the skin and in contact with body fluids (*e.g.*, interstitial fluid). Also, they provide a high drug loading capacity and tunable drug release rate based on the polymer crosslinking ratio, which is used for HFM preparation.[11] HFMs are used in different applications such as interstitial fluid extraction and analysis, therapeutic agent delivery, skin cancer treatment, and wound healing.[12,13]

1.1.5. Dissolving MNs. Dissolving MNs enable the release of therapeutic agents or vaccines incorporated into MNs which are made from safe biomaterials, such as biodegradable or biocompatible natural or synthetic polymers.[2] Dissolving MNs enable the release of encapsulated pharmaceutical agents painlessly and gradually.[7,9]

Dissolving MNs are more prominent than the other forms of MNs in terms of therapeutic efficacy and the penetration of carriers.[2]

Metals (steel, titanium, nickel), polymers (poly-glycolic acid (PGA), polylactide-*co*-glycolic acid (PLGA), poly-L-lactic acid (PLA), chitosan), glass, silicon, ceramics and carbohydrates (trehalose, sucrose, mannitol) are utilized to make MNs for therapeutic uses.[14] Because of their distinct features, PLGA-based carriers are considered viable methods for MN systems.[15,16]

1.2. PLGA as a nanocarrier and main polymeric matrix for MNs

Colloidal materials such as natural macromolecules and synthetic polymers have been widely exploited in the manufacture of nanoparticle-based complexes for drug delivery.[17,18] Natural polymers are purer than synthetic polymers. However, synthetic polymers such as PLGA, PLA, polycaprolactone (PCL) and PGA are widely used in nanocarrier formulations due to their biocompatibility and biodegradability.[17,19] PLGA is an FDA-approved biodegradable copolymer that hydrolyzes in the body in the presence of water and creates the original monomers, lactic acid and glycolic acid. Under normal physiological conditions, these monomers are also byproducts of various metabolic pathways. In the body, these degradation products are easily metabolized and removed through the Krebs cycle. As a result, the systemic toxicity associated with employing PLGA for drug delivery or any other biomaterial application is minimal and negligible.[20] PLGA is commonly used in clinical applications, mainly for targeted drug delivery.[21,22] The biosynthesis and structure of PLGA are shown in Fig. 2. PLGA has high biocompatibility, biodegradability and unique adsorption capabilities.[23,24] It is widely utilized as a delivery nanocarrier for proteins, medicines and other molecules like peptides, RNA and DNA. It can be loaded in different types of MN patches and provide a long-term transdermal drug delivery profile through the PLGA nanocarriers.[23,25,26] Due to the degradation of PLGA, it has lately been revealed that it can be employed for sustained drug release in optimal amounts *via* implantation and without surgery. It can also be used as the main MN matrix, embedded with various therapeutic formulations.[22,26–28]

Furthermore, the overall physical features of the polymer–drug matrix can be modified based on the drug, preferred dose and start-release period by adjusting relevant factors, including polymer molecular weight, lactide/glycolide ratio and drug concentration.[23,29] The surface functionalization of PLGA nanoparticles with specific ligands, including aptamers, peptides and other polymers, results in a tailored colloidal nanocarrier that can escape the reticuloendothelial system and

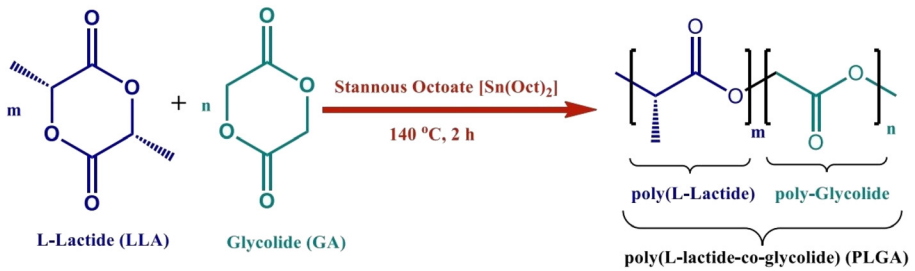

Fig. 2 Synthesis and structure of PLGA. Reproduced from ref. 34 with permission from MDPI, copyright 2021.

select a particular receptor in the targeted site.[30,31] This also decreases non-specific body cell contact and adsorption of PLGA nanoparticles.[32] Numerous PLGA-based nanocomplexes were recently developed to transport various medicinal treatments. Porous MNs composed of PLGA were tested for interstitial fluid sampling.[33] Even if MNs break down upon injection into the skin, the PLGA MN array has the advantage of not remaining in the skin. As a result of the limited invasiveness and safety, it is likely to be extensively used for diagnostic devices.[33]

2. Preparation of PLGA-based MNs

Most PLGA-based MNs are made *via* multi-step micromolding, as shown in Fig. 3.[3,35] PLA, PGA, and PLGA-based microparticles are generally prepared using spray drying and emulsion procedures. Then polymeric microparticles are placed in polydimethylsiloxane (PDMS) micromolds and used to create polymeric MNs through micromolding.[36] Rapidly prototyping biodegradable PLGA MN arrays have also been accomplished using an integrated approach of swift and low-cost CO_2 photolithography and polymer shaping.[37]

While micromolding processes ensure excellent tip resolution and repeatability, they require extensive processing steps, have poor degrees of system engineering, are a source of potential impurities, and cannot be employed with thermo-sensitive drugs, especially for hot embossing and injection micromolding. The current tendency is to create MNs using mold-free procedures to meet market demands. For the production of PLGA biodegradable MNs, electro-drawing is presented as a rapid, low-temperature, one-step alternative to mold-based methods. In the novel electro-drawing strategy, titanium micro-heaters are embedded onto the pyroelectric surface.[38] The plasticity of the electro-drawing technology and the water-in-oil (W/O) precursor emulsion method modify the drug release profile of MNs.[39]

A robust approach for producing mass-customizable master molds is pre-drying and chip casting to create sharp-tipped biodegradable polymeric MNs. The method's usefulness was demonstrated by constructing dissolving PLGA MNs for drug delivery and conducting pig skin permeation and *in vitro* degradation tests.[40] Microlens technology can also create tapered MN arrays by utilizing UV lithography without requiring complicated equipment or advanced controls. The prepared PLGA MN arrays cloned from a negative PDMS master effectively penetrated mouse skin.[41]

It should be noted that manufacturing conditions such as highly concentrated formulations, high temperatures and extended drying times frequently used in producing drug-

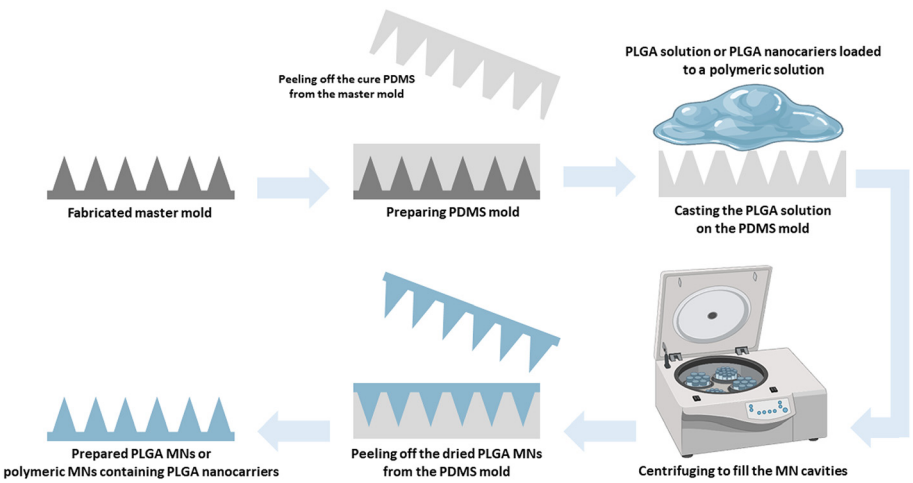

Fig. 3 Schematic illustration of the PLGA MN preparation method.

loaded polymeric MNs can cause adverse drug stability in MNs. Using organic solvents and solubilization can also drastically reduce the stability of labile compounds in biodegradable polymer matrices. A study showed that incorporating bovine serum albumin (BSA) into water-soluble polyvinyl alcohol (PVA) and biodegradable PLGA MNs using a dual-nozzle spray deposition technique could improve drug stability.[42]

3. Transdermal delivery of PLGA-based MNs

Polymeric materials have the potential to be used in a wide range of innovative technologies. Integrating molecules and drugs into PLGA polymer matrices, which create polymeric nanocarriers, has sparked great interest for applications in drug delivery.[43] Along this line, the use of polymeric MNs is a promising method for transdermal drug delivery.[44,45] MNs penetrate the skin's SC barrier layer, allowing therapeutic agents to penetrate deeper into viable skin areas without triggering pain receptors or causing vascular injury. Fig. 4 compares the drug delivery efficiency of MN transdermal patches with other mechanisms of transdermal drug delivery systems. It is also reported that flexible PLGA MN meshes, such as naturally biocompatible silk fibroin (SF) protein, considerably increase drug delivery efficiency compared to a stiff form.[46]

In the last decade, PLGA MNs modified with dyes or florescent agents have been used to track the MN-mediated delivery of loaded components through the skin (Table 1). For example, in a Franz diffusion cell, the observation of double fluorescent PLGA nanoparticles in mouse skin revealed the role of MNs in penetration and transdermal improvement.[47]

The penetration of PLGA-based MNs into shaved mouse skin was also demonstrated by coumarin 6 and R-phycoerythrin as fluorescent probes. The results revealed that MNs enhanced the number of nanoparticles deposited in the skin. It was also confirmed that particle size substantially

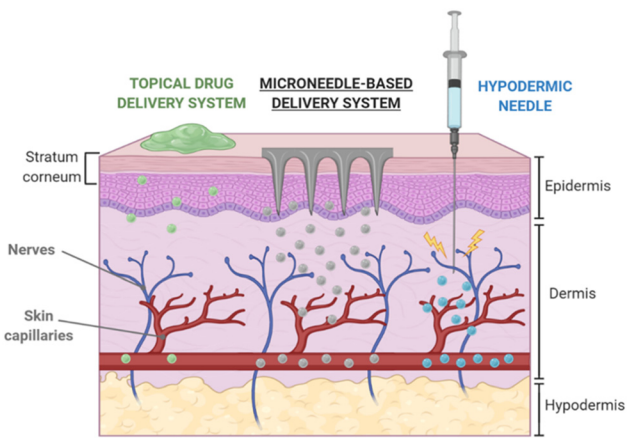

Fig. 4 Transdermal delivery *via* MN-based platforms in comparison with other routes. Reproduced from ref. 9 with permission from MDPI, copyright 2020.

Table 1 Tracking of the transdermal delivery of PLGA-based MNs

Type of MNs	Design strategy	Tracking agents	Skin sample (animal model)	Ref.
Dissolving MNs	Nile red/copolymer Gantrez® AN-139/ PLGA MN array	Nile red	Porcine	49
	RhB/PLGA MNs	RhB	Porcine ears	50
	RhB/FITC/PLGA MN array	RhB and FITC	Porcine	51
	Hydrophobic PLGA MNs	RhB	Porcine	52
	Dexamethasone-coated MNs	RhB or FM1-43	Mice, rats, porcine	53
Hollow metal MNs	Nickel/PLGA MNs	Sulforhodamine B	Porcine and hairless guinea porcine skin	55

impacted the penetration and distribution of MNs.[48] Donnelly *et al.* reported MN-based transdermal delivery by a model hydrophobic dye, Nile red. Nile red was placed into polymeric MN arrays made from aqueous blends of the mucoadhesive copolymer Gantrez® AN-139 and inserted into PLGA nanoparticles. Following MN administration, tissue permeation assays utilizing excised pig skin indicated substantial tissue concentrations of Nile red.[49] A MN-based method was used by Gomaa *et al.* to demonstrate the high transdermal distribution of rhodamine B (RhB) encapsulated in PLGA nanoparticles in full-thickness porcine skin.[50] RhB and fluorescein isothiocyanate (FITC) were packed into PLGA nanoparticles and administered to full-thickness pig skin pretreated with a MN array.

The physicochemical properties of the nanoparticles and the encapsulating colors influenced penetration into the MN-treated skin. In the case of enclosed dyes, solubility at physiological pH and possible interaction with skin proteins were more important factors for skin penetration than molecular mass.[51] Lee *et al.* discovered that hydrophobic heat-melted PLGA dissolvable MNs could be implanted into *ex vivo* pig skin effectively, releasing RhB nearly four weeks after the MNs were implanted (Fig. 5).[52] The release of medications from polymeric MNs into the inner ear was demonstrated by the preparation of PLGA MNs loaded with RhB or FM1-43 dye.[53]

In MN-based transdermal delivery, the spontaneous repair of pores arising from PLGA-based MNs was found to be a significant factor that could prevent the burst release of loaded molecules, drugs or therapeutic agents. Pore recovery is thought to be triggered by high surface tension in the films and viscoelastic creep. Bigger pores require more time to heal than smaller pores.[54] These findings suggest that combining PLGA nanoparticles with MNs could be a good way to improve topical medication administration and therapy by providing drug reservoirs to the skin.

In conclusion, PLGA-based MNs offer several advantages for transdermal drug delivery. These MNs can potentially deliver a wide range of drugs with varying molecular weights, including hydrophilic and lipophilic drugs. They can also bypass the stratum corneum, the primary barrier to drug delivery through the skin; this results in improved drug delivery

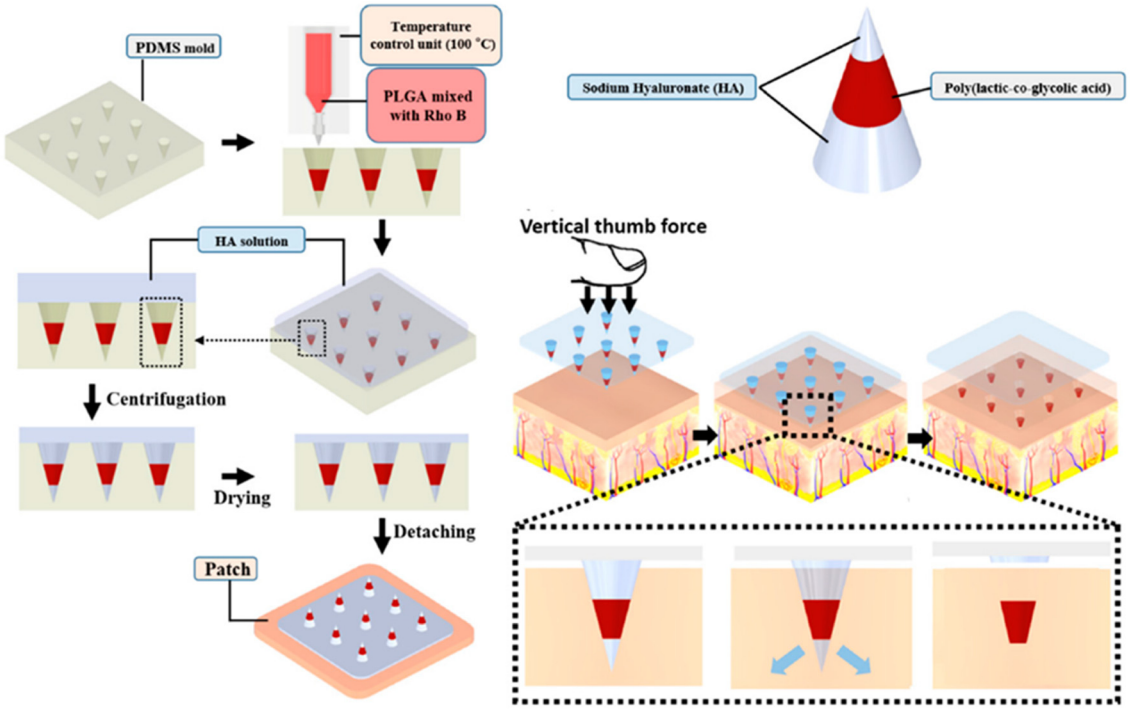

Fig. 5 Schematic illustration of the preparation process of PLGA-based MNs and the dye-based tracking of transdermal delivery. Reproduced from ref. 52 with permission from MDPI, copyright 2021.

efficiency and bioavailability, with reduced side effects. Furthermore, using PLGA, a biocompatible and biodegradable polymer, ensures the safety of these MNs *in vivo*. In addition, the ease of manufacturing, storage, and administration of PLGA-based MNs makes them a promising alternative to traditional drug delivery methods. Overall, PLGA-based MNs have significant potential to enhance the field of transdermal drug delivery and improve patient outcomes. The following sections discuss the applications of PLGA-based MNs.

4. PLGA-based MN applications

4.1. Vaccine delivery

Vaccination is frequently utilized to promote human health as it is the most cost-effective and best preventative technique for treating several diseases.[56] However, most vaccines are currently administered *via* injection, which has several drawbacks, including the requirement for inoculation by specialists, discarded metal needle contamination and infection, and low vaccination adherence.[57,58] To overcome these limitations, a number of MNs have been created during the last two decades. They are being used to administer vaccines due to their convenience and effectiveness over alternative drug carriers.[3,8,59] In particular, the biocompatible micro/nanoparticle (liposome, polymeric nanoparticle and hydrogel)-constituted MN arrays are an effective and consistent vaccine adjuvant-delivery system. These MNs enable painless vaccination by minimally trained workers or self-administration *via* the cutaneous or mucosal routes.[60] Table 2 presents prominent examples of prepared PLGA MNs for vaccine delivery.

4.1.1. Vaccine delivery by PLGA-based hollow MNs. The prevalence of a significant number of epidermal and dermal antigen-presenting cells makes the skin an appealing organ for immunization.[9] Vaccines can be delivered to the skin in an accurate and non-invasive manner using hollow MNs. Utilizing hollow MNs, Du *et al.* examined the ability of intradermal administration of nanoparticle-based vaccinations to alter the immune response of protein antigens. A prototype antigen (ovalbumin (OVA)) was loaded with and without an adjuvant TLR3 agonist, poly(I:C), into four types of nanoparticles: PLGA nanoparticles, liposomes, mesoporous silica nanoparticles (MSNPs), and gelatin nanoparticles (GNPs). A hollow-MN patch was used to effectively inject nanoparticle suspensions into mouse skin at a depth of roughly 120 μm. Strong total IgG and IgG1 responses were evoked by the OVA/poly(I:C)-loaded nanoparticles. In contrast to the OVA/poly(I:C) solution, co-encapsulation of OVA and poly(I:C) in nanoparticles dramatically boosted the IgG2a response. IgG2a responses were higher in PLGA nanoparticles and liposomes than in MSNPs and GNPs. In addition, OVA/poly(I:C)-loaded liposomes produced the most $CD8^+$ and $CD4^+$ T cell responses (Fig. 6(a)).[61]

In another study, hollow MNs were used to deliver OVA-loaded PLGA nanoparticles intradermally with and without poly(I:C). The PLGA nanoparticles triggered a cytotoxic T-cell response, which could protect cells from intracellular infections. De Groot *et al.* found that a single injection of OVA-loaded PLGA nanoparticles stimulated both adoptively trans-

Table 2 PLGA-based MNs for the delivery of various vaccines

Type of MNs	Design strategy	Vaccine candidate	Effects	Ref.
Hollow MNs	OVA/poly(I:C)/PLGA nanoparticles	Intradermal vaccine	Enhanced IgG2a, $CD8^+$ and $CD4^+$ T cell responses	61
	OVA/poly(I:C)/PLGA nanoparticles	Intracellular infections	Enhanced $CD8^+$ and $CD4^+$ T cell responses	62
	OVA/imiquimod and monophosphoryl lipid A/PLGA nanoparticles	Intradermal vaccine	Generated a much larger IgG2a response and a higher number of IFN-γ secreting cells	63
Dissolving MNs	PAA/PLGA/MN arrays	A subunit vaccine	The improvement of cellular immunity	56
	OVA/poly(I:C)/PLGA nanoparticle loaded hyaluronan MNsOVA/PLGA MNs	Intracellular infections Antigen expressing B16 melanoma tumors and parainfluenza	Enhanced $CD8^+$ and $CD4^+$ T cell responses The proliferation of antigen-specific T cells Induced efficient antitumor and anti-viral immune responses	65 64
	Ebola DNA/PLGA-PLL/γPGA MNs	Ebola DNA vaccine	Improved vaccine thermostability and immunogenicity	66
	Luciferase-expressing plasmid/PRRSV/PLGA MNs	Important clinical swine arterivirus	Stimulated anti-PRRSV IgG responses	67
	HPV-Q particles/PLGA MNs	Human papillomavirus (HPV)	Produced IgG	68
	Influenza M2 antigen/PLGA MNs	Influenza	A dual-delivery system for immunization	69
	PLP139–151 peptide/PLGA MNs	Anti multiple sclerosis	Antigen-specific therapy	70
	PSS/PAH/PLGA gelatin nanoparticle MNs	Tetanus toxoid	Immuno-protection against tetanus toxoid	71
	OVA/poly(I:C)/nanoparticle MNs	Intradermal vaccine	Enhanced IgG2a, $CD8^+$ and $CD4^+$ T cell responses	65
Coated/solid MNs	pDNA/PLGA/PEG/PLGA hydrogel MNs	Intradermal DNA vaccination	MN-assisted transport of pDNA to skin	73
	pDNA/PLGA MNs		Improved immune responses	74
	pDNA/PLGA/PEI polyplex MNs		Generated a higher humoral immune response	75

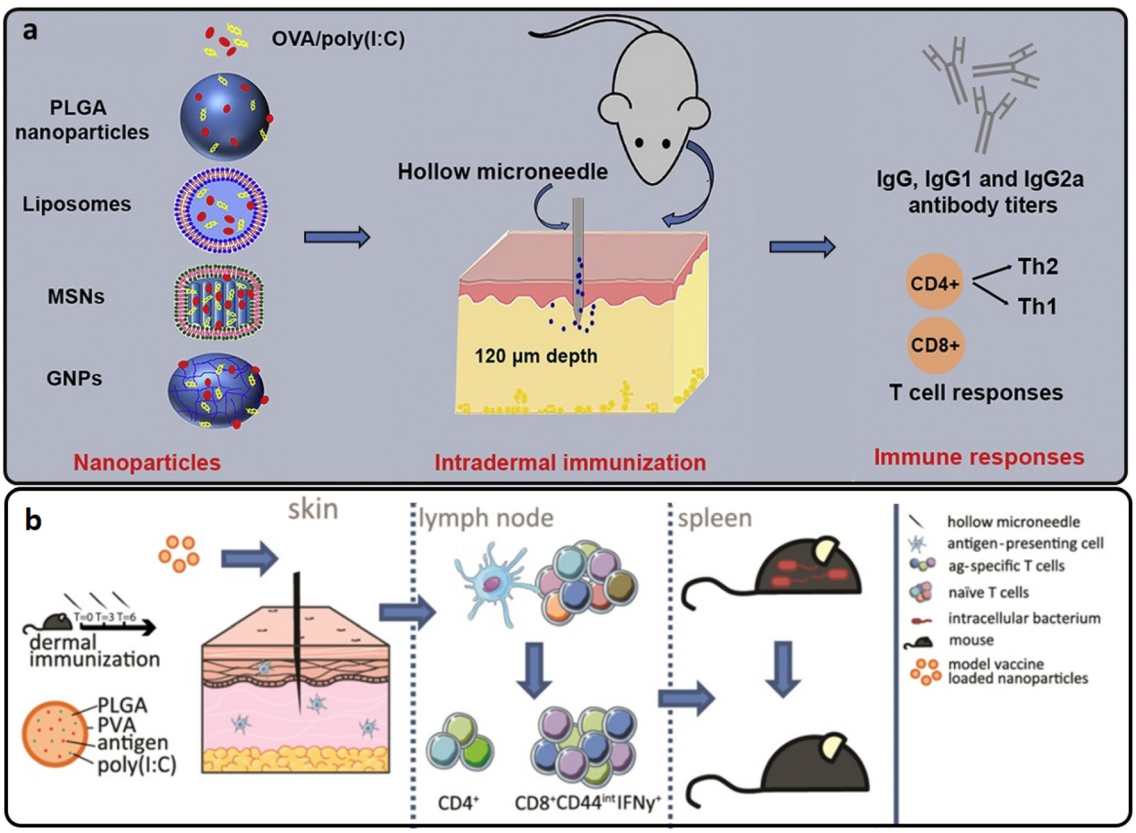

Fig. 6 (a and b) The intradermal vaccination process of OVA-loaded into PLGA hollow MNs. Reproduced from ref. 61 and 62 with permission from Elsevier, copyright 2017.

planted antigen-specific naive transgenic $CD8^+$ and $CD4^+$ T cells with significantly higher effectiveness than soluble OVA. PLGA nanoparticles stimulated endogenous OVA-specific $CD8^+$ T lymphocytes using a triple vaccination regimen (Fig. 6(b)). After immunization with anionic PLGA nanoparticles co-encapsulated with OVA and poly(I:C), the immune response conferred resistance against a recombinant strain of the intracellular bacteria *Listeria monocytogenes* that secreted OVA.[62]

Niu *et al.* evaluated the use of the hollow MN array for polymeric nanoparticle intradermal administration in rats. Intradermal distribution of polymeric nanoparticles through a hollow MN array produced a distinct pharmacokinetic profile defined by an early burst transit *via* the draining lymph nodes and a very limited overall systemic exposure compared to intravenous and subcutaneous methods of administration. The vaccine composition included a model antigen, OVA, TLR agonists, imiquimod and monophosphoryl lipid A encapsulated in PLGA nanoparticles. Antigen-loaded nanoparticles from a hollow MN array generated a much larger IgG2a antibody response and a higher number of IFN-γ secreting cells, both Th1 response biomarkers.[63] Therefore, hollow MN-mediated intradermal administration of polymeric nanoparticles is feasible for developing vaccine formulation efficacy.

4.1.2. Vaccine delivery by PLGA-based dissolving MNs. In a study, controlled-release polymer depots were implanted into epidermal tissue using a dissolving MN array. A water-soluble poly(acrylic acid) (PAA) matrix was used to create MN arrays made of drug-loaded PLGA MNs or solid PLGA tips. When MNs were applied to the skin of mice, they easily penetrated the SC and epidermis. After penetrating the exterior layers of the skin, the PAA binder quickly dissolved in contact with the epidermis' interstitial fluid, thereby inserting the MNs into the tissue. These polymer depots stayed in the epidermis for weeks after implantation, allowing encapsulated cargoes to be released for systemic administration. The capacity of these composite MN arrays to carry a subunit vaccine composition proved the efficacy of this method.[56]

Antigen transport to antigen-presenting cells, particularly dendritic cells (DCs), and subsequent activation of these cells continue to be a noticeable problem in creating successful vaccines. A study highlighted the potential of dissolving MN arrays packed with nano-encapsulated antigens to enhance vaccination immunogenicity by targeting antigens to consecutive DC pathways within the skin. The skin-resident DCs could transfer OVA-encapsulated PLGA nanoparticles to epidermal draining lymph nodes after *in situ* absorption, resulting in the considerable proliferation of antigen-specific T cells. Through the stimulation of antigen-specific cytotoxic $CD8^+$ T cells, which led to effective tumor and viral clearance, this method offered complete immunity *in vivo* against the emergence of antigen-expressing B16 melanoma tumors and a mouse model of parainfluenza (Fig. 7(a)). As a result, using biodegradable PLGA nanoparticles for preferential antigen targeting to skin DC subsets *via* dissolvable MNs is viable technology for enhanced vaccination effectiveness.[64] A study, investigated dissolving MNs fabricated from hyaluronan loaded with PLGA nanoparticles co-encapsulating OVA and ploy (I:C) and compared them to their previous study using hollow MNs.[62] Immunization with free antigens in dissolving MNs produced comparable immune responses to administration through hollow MNs. Nevertheless, the humoral and cellular immune responses induced by nanoparticle-loaded dissolving MNs were inferior to those induced by nanoparticles given *via* a hollow MN.[65]

Also, some researchers have focused on the transdermal delivery of anti-viral vaccines *via* MN platforms. For instance, the Ebola DNA vaccine was embedded in PLGA-PLL/γPGA nanoparticles and applied to the skin with MNs (Fig. 7(b)). The nanoparticle/MN-based delivery improved vaccine thermostability and immunogenicity compared to a free vaccination. Immune responses were stronger when MNs were used instead of intramuscular injections.[66] Bernelin-Cottet *et al.* assessed the efficacy of dissolvable MNs for arterivirus vaccine DNA administration in pigs by intradermal injection with surface electroporation (EP) and PLGA nanoparticle MNs. They used a luciferase-expressing plasmid as a reporter and plasmids encoding antigens from PRRSV, an important clinical swine arterivirus. Although at a lower level than EP, patches successfully generated luciferase expression in the skin. EP treatment elicited anti-PRRSV IgG responses that were not seen with MNs. The results of this study showed that electroporation and MNs could be used to administer DNA vaccines to pigs' skin successfully.[67]

The human papillomavirus (HPV) is a sexually transmitted pathogen that causes most cervical cancer cases. HPV vaccination rates are still low due to the necessity for several doses, leading to low compliance and ineffective protection. Shao *et al.* employed a scalable production method to manufacture implantable polymer–protein mixes for single administration with controlled delivery to overcome the disadvantages of the current HPV vaccinations. To improve the immunogenicity of virus-like particles generated from bacteriophage Q, peptide epitopes from HPV16 capsid protein L2 were attached to them. Following this, the HPV-Q particles were loaded into PLGA implants. In a pseudovirus neutralization test, mice vaccinated with the HPV-Q implants produced IgG titers equivalent to those produced by standard soluble injections.[68]

Braz *et al.* aimed to produce fast-dissolving MNs that could transport antigen-loaded controlled-release polymeric nanoparticles *via* the skin resulting in a dual-delivery system for immunization. The technology employs prompt-dissolving MNs loaded with PLGA nanoparticles to package a model influenza matrix 2 (M2) protein antigen and then quickly dissolve, releasing the antigen-laden nanoparticles (Fig. 7(c)). The antigen-loading effectiveness and dissolvability of the lead M2 PLGA nanoparticle-loaded dissolvable MN patch formulation was validated on murine and porcine skin. The research resulted in an antigen nanoparticle-loaded dissolvable MN platform for transdermal vaccine delivery that was simple to make, well-characterized and translatable.[69]

Specific antigens are being investigated to re-establish immunological tolerance, particularly in the context of mul-

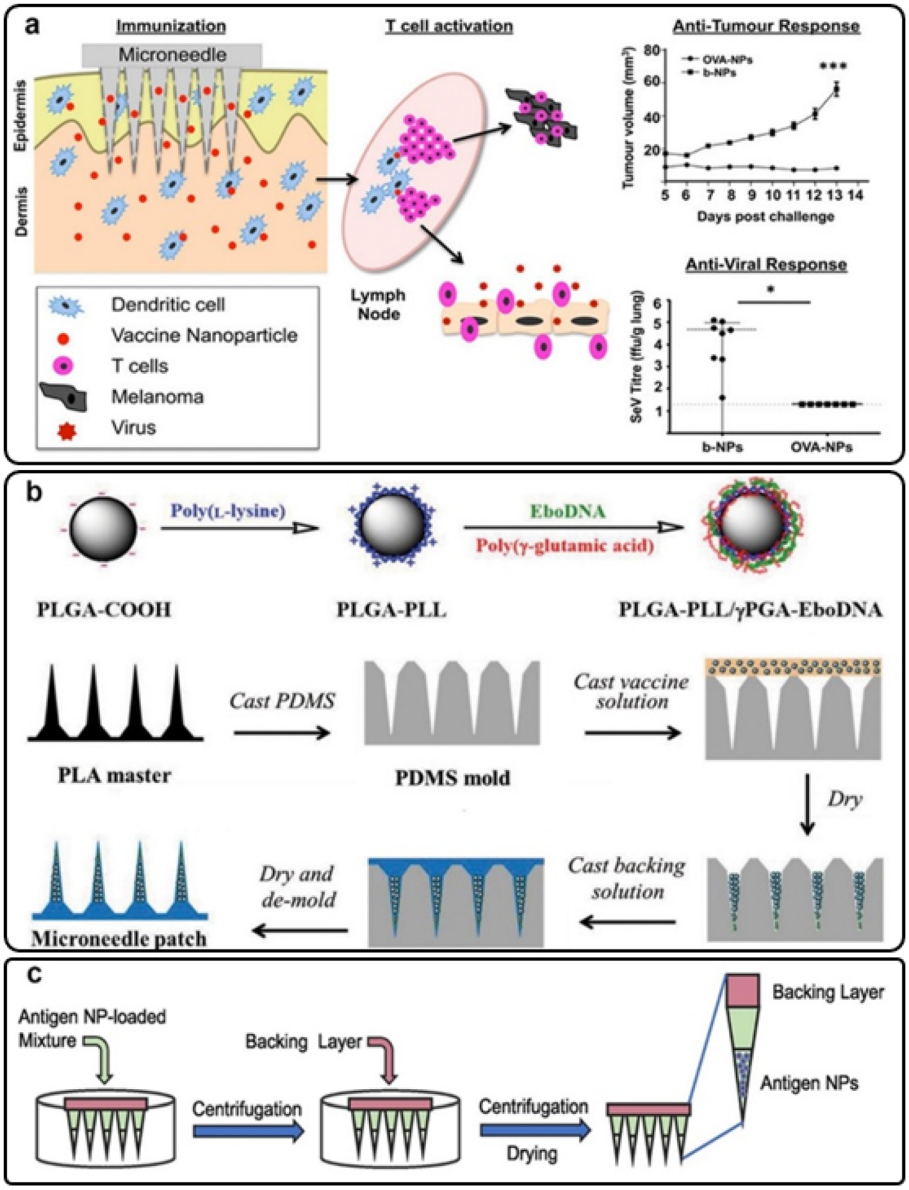

Fig. 7 (a) Antitumor and anti-viral immune responses of skin dendritic cells targeted *via* PLGA MNs; reproduced from ref. 64 with permission from ACS, copyright 2013; (b) the preparation procedure for PLGA-PLL/γPGA-EboDNA dissolving MNs; reproduced from ref. 66 with permission from Wiley, copyright 2017; (c) influenza matrix 2 (M2) antigen nanoparticle-loaded PLGA MNs; reproduced from ref. 69 with permission from Elsevier, copyright 2022.

tiple sclerosis (MS). PLP139-151 is a proteolipid protein (PLP) peptide, myelin's most common protein, which is found to be a potent tolerogenic molecule in MS. The peptide was encapsulated in PLGA nanoparticles and then incorporated into polymeric MNs to ensure efficient transport of the nanoparticles and peptide into the skin, which is a highly immune-active organ. PLP-loaded PLGA nanoparticles showed a size range of 200 μm and more than 20% encapsulation effectiveness. PLP was released from the nanoparticles within the first few hours of incubation in a physiological medium. When the nanoparticles were loaded into MNs, structures with a height of 550 μm and a diameter of 180 μm were created. The findings suggest that this technique could be used to combine a novel antigen-specific therapy in the setting of MS, allowing for the injection of PLP-loaded nanoparticles into the skin with little invasiveness.[70]

Another study reported the immunopotentiation activity of a soluble MN array containing tetanus toxoid nanoparticles without any adjuvant. The gelatin nanoparticles were made from polystyrene sulfonate (PSS), polyallylamine hydrochloride (PAH), and PLGA in a layer-by-layer coating process. Afterwards, the filtered gelatin nanoparticles were disseminated in aqueous PVP K10 fluid and incorporated into a mold to create MNs. For 8 hours, gelatin nanoparticles followed a continuous release pattern, whereas nanoparticle-loaded dissolvable MNs followed a controlled release profile for

24 hours. The strongest antibody synthesis in response to tetanus toxoid was seen in amine-modified nanoparticle-based MNs. As a result, tetanus toxoid can be delivered using nanoparticulate dissolvable MN-based immunopotentiation.[71] MN administration provides much better cellular immunity and equal development of serum antibodies compared to standard needle-based immunization, indicating the promise of the dissolvable MN technique for vaccine delivery.

4.1.3. DNA vaccine delivery by PLGA-based coated/solid MNs. A DNA vaccine is a promising technique due to its well-established production process, safety, adaptability to quickly address the pandemic of viruses and stability at room temperature.[72] An optimal DNA delivery route has yet to be found along this line. Recently, MNs have opened new prospects for resolving the problem of inaccurate DNA vaccine delivery. The administration of nucleic acids through the skin has a variety of medicinal uses, the most notable of which is genetic vaccination. Non-viral gene expression in the skin is, unfortunately, poor and temporary. In a study, by integrating MN delivery technology with sustained-release plasmid DNA (pDNA) hydrogel formulations, the possibility of pDNA delivery through the skin was investigated.[73] Wet etching of silicon in potassium hydroxide was used to make the MNs. Carbopol polymers and thermosensitive PLGA-PEG-PLGA triblock copolymers were utilized to make the hydrogels. MN penetration and pDNA diffusion were studied using freshly excised human skin. After MN therapy, channels of about 150–200 μm depth enhanced transepidermal water loss in the skin. The pDNA hydrogels slowly released the pDNA. The pCMV reporter gene was expressed in the viable epidermis following MN-assisted transport of pDNA hydrogels through human skin.[73] The study showed that MN-mediated transcutaneous pDNA immunization had the potential to elicit a more significant immune response than intramuscular pDNA injection. In another study, Kumar *et al.* found that coating pDNA on the surface of PLGA as cationic nanoparticles dramatically improved the immune response caused by transcutaneous vaccination by putting pDNA onto a skin region prepared with solid MNs. Transcutaneous vaccination with pDNA-coated net positively charged nanoparticles induces a greater immunological response than intramuscular immunization with pDNA alone or with pDNA-coated net negatively charged nanoparticles.[74]

Although intradermal DNA vaccination is a potential immunization technique, DNA vaccines are hard to deliver to target cells in the skin by polyplexes. Seok *et al.* described how MNs covered with a polyplex comprising PLGA/polyethyleneimine (PLGA/PEI) nanoparticles could be used to facilitate intradermal pH1N1 DNA vaccine delivery (Fig. 8). The polyplex encapsulating pDNA vaccine was coated onto stainless steel MNs with increased hydrophilicity (N/P ratio of 6 : 1 and no dispersion) and covered with the polyplex encapsulating pDNA vaccine (N/P ratio of 6 : 1 and no aggregation). Compared to intramuscular polyplex delivery or bare pH1N1 DNA vaccine delivery *via* a dry-coated MN, the covered polyplex quickly dissolved in pig skin within five minutes and generated a higher humoral immune response. These findings suggest that skin vaccinations might benefit from intradermal administration of pDNA vaccines inside a cationic polyplex coated on MNs.[75]

4.2. Drug/therapeutic agent delivery

4.2.1. Anti-cancer agent delivery by PLGA-based MNs. Recurrent cancers, especially oral carcinoma, are hard to treat

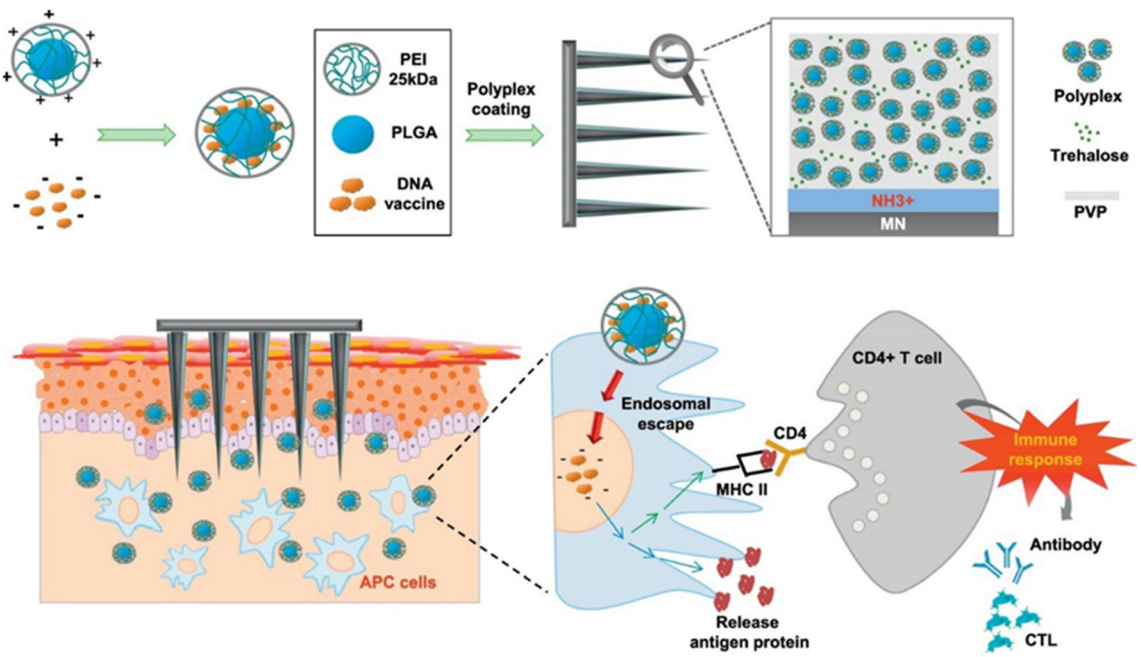

Fig. 8 The intradermal delivery of pH1N1 DNA by MNs covered with a polyplex comprising PLGA/PEI nanoparticles as a DNA vaccine platform. Reproduced from ref. 75 with permission from Elsevier, copyright 2017.

as standard surgical techniques are ineffective for these patients.[76] Furthermore, systemic chemotherapy does not work effectively for many individuals.[77] Anti-cancer medications injected locally intratumorally are considered an appealing alternative therapeutic option for these individuals.[78,79] Traditional hypodermic administrations result in poor drug distribution in the tumor and drug leakage from the injection site into the circulatory system, leading to discomfort for the patient.[80] Some research aimed to create MNs as a new method for direct and less invasive intradermal anticancer agent administration (Table 3).

Among chemotherapeutics, doxorubicin (DOX) is one of the most used drugs in various cancer therapy approaches.[81,82] DOX-encapsulated PLGA nanoparticles were produced and coated on MNs. MN arrays coated with DOX-PLGA nanoparticles to treat swine cadaver buccal tissue indicated that DOX might penetrate vertically and laterally into the tissues and cause cellular cytotoxicity. The administration of various quantities of hypodermic fluid into porcine buccal tissue revealed considerable leakage of the injected volume (about 25%). This work shows that drug-coated MNs are an appealing microscale technology for consistently and effectively delivering medications to localized cancer.[76]

Nguyen and Banga examined *in vitro* methotrexate distribution in the dermatomed porcine ear and human cadaver skin treated with PLGA MNs or fractional ablative laser. Then, an *in vitro* penetration test was confirmed using Franz diffusion cells. The PLGA MNs enhanced the *in vitro* transdermal delivery of methotrexate into and across the skin markedly.[83] MN transdermal patches combine hypodermic needles with transdermal patches to address the limitations of both administrations and patches alone. Biodegradable PLGA recombinant human keratinocyte growth factor (rHuKGF) MNs were prepared by micromolding. In total, MNs with a height of 600 μm and a base of 300 μm were created and loaded with rHuKGF. *In vitro*, the medication from the MNs was secreted for 30 minutes. According to this study, the strength of the MNs in the patch was good, as MNs could reach 381 μm into the parafilm without any structural changes or fracturing. This might have therapeutic implications with benefits such as lower dose frequency, enhanced patient compliance and increased bioavailability.[84]

Furthermore, Li *et al.* developed a MN patch encapsulated with chimeric antigen receptor T cells (CAR T cells), which enabled *in situ* penetration-mediated seeding of CAR T cells in tumor beds or cavities following surgical resection. CAR T cells loaded into the pores of the MN tips were efficiently and uniformly delivered to the tumor without losing their activity. Compared to direct intratumoral injection, CAR T cell infiltration and immunostimulatory capacity were improved by MN-mediated local administration. This customizable patch provides a novel platform for the dispersed seeding of live cells to treat a broad range of tumors[28] (Fig. 9).

4.2.2. Diabetes-related medication delivery by PLGA-based MNs. The metabolic disorder diabetes is characterized by hyperglycemia.[22] Integrating nanoparticles as a selective drug

Table 3 PLGA-based MN delivery of various drug/therapeutic agents, vitamins and proteins

Delivery agents	Type of MNs	Design strategy	Drug/therapeutic agents	Animal skin model	Ref.
Anti-cancer agents	Coated MNs	DOX/PLGA coated on MNs	Doxorubicin (DOX)	Porcine	76
	Dissolving MNs	Methotrexate/PLGA MNs	Methotrexate		83
		Recombinant human keratinocyte growth factor (rHuKGF)/PLGA MNs	rHuKGF		84
		Chimeric antigen receptor T cell (CAR T)/PLGA porous MNs	CAR T cell	Mice	28
Diabetes-related medication	Dissolving MNs	Insulin-loaded PLGA MNs	Insulin	Mice	85
		Liraglutide (Lira) encapsulation in PLGA nanoparticles	Liraglutide (Lira)	Rats	86
		Collagen type III and naproxen-loaded PLGA/HA MNs	Recombinant collagen type III Naproxen (Nap)		89
Anti-infection agents	Dissolving MNs	PLGA-based hydrogel-forming MN bases (HFMBs)	Amphotericin B	Porcine	91
		Tenofovir-loaded PLGA MNs	Tenofovir alafenamide (TAF)	Rat	95
Hormonal drugs	Dissolving MNs	*N*-Methyl pyrrolidinone/PLGA MNs	Etonogestrel (ENG)	Rat	45
		Implantable PLGA MNs with detachable HA backing layer	β3-Adrenoceptor agonist and thyroid hormone T3		102
		Implantable PLGA MNs loaded with LNG	Levonorgestrel (LNG)		27
		Separable PLGA MNs loaded with LNG			98–100
	Coated MNs	Thermostable hydroxypropyl methylcellulose (HPMC)/PLGA MNs			101
Other drugs	Dissolving MNs	Biocompatible fentanyl (Fen)-bearing PLA/PLGA nanoparticle MNs	Fentanyl	Mice	105
		A mixture of diltiazem pH-responsive PLGA nanospheres/nifedipine-PVP	Nifedipine and diltiazem	Rat	106
		Injectable PLGA MNs	Finasteride (FND)	Porcine	108
		Detachable hybrid MN depot PLGA shell filled with GelMA–MSC mixture	Mesenchymal stem cells (MSCs)	Mice	109
	Coated MNs	PEI/PLGA/stainless steel MNs	Lidocaine	Porcine	110
		PLGA porous-coated MNs			111

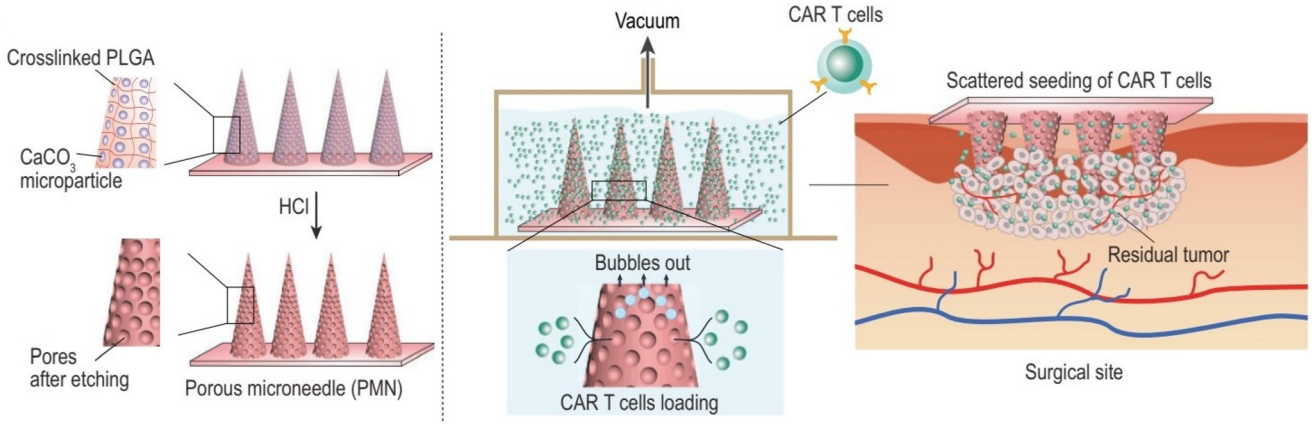

Fig. 9 Porous MN characterization for CAR T cell loading and administration into the tumor bed post-surgery. Reproduced from ref. 28 with permission from Oxford University Press, copyright 2021.

carrier with non-invasive dissolving MNs could be a potential approach for future diabetes therapeutic agent delivery (Table 3). Yang *et al.* presented a new PLGA-based dissolved MN patch with electrospinning PLGA solution (14% w/v), delivering insulin loaded on MNs into the skin of a healthy mouse model quickly. This dissolvable MN array addressed significant concerns related to the low permeation efficiency of MNs.[85] In another study, liraglutide (Lira)-encapsulated PLGA nanoparticles were encapsulated into the MNs, showing 15 days of continuous release of Lira in a biphasic profile with 80% of the content being released in the first eight days. This platform eliminated the need for subcutaneous Lira injection by embedding sustained-release nanoparticles into MNs containing 50% PVP w/v.[86]

Chronic diabetic wounds are now a significant burden on patients and the healthcare system.[87,88] Chronic wound healing is substantially hampered by persistent inflammation and inadequate tissue remodeling.[87] For chronic diabetic wound therapy, recombinant humanized collagen type III (rhCol III) and naproxen (Nap) loaded PLGA nanoparticles incorporating HA MNs were created. Customized rhCol III showed significant cell adhesion because it was made from the Gly483-Pro512 section which included the highly sticky segments (GER, GEK) in the human collagen type III sequence. Within minutes, rhCol III and Nap@PLGA nanoparticles were immediately released into the wound area. The produced MNs had good biocompatibility and promoted efficient fibroblast and endothelial cell proliferation and migration. Additionally, the *in vivo* regeneration potential of synthesized MNs was demonstrated using a diabetic rat full-thickness skin wound model. The results showed that MNs may speed up wound repair by lowering inflammation and boosting angiogenesis or collagen deposition.[89]

4.2.3. Anti-infection agent delivery by PLGA-based MNs. MN devices are demonstrated to be a unique and intriguing intradermal anti-infection agent administration method that can be useful for continuous release (Table 3).[90] For example, Peng *et al.* developed a unique hybrid MN patch with implantable PLGA tips matched with hydrogel-forming MN bases (HFMB). In a regulated way, Nile red (a model dye) and amphotericin B (an antifungal medication) were injected into PLGA tips. Adding the pre-formed HFMB (MN8) to the standard solubility baseplate (MN0)-based PLGA-tipped implantable MN configuration enhanced the *in vitro* and *ex vivo* implantation capacities of the patches. It also increased *ex vivo* drug delivery efficiency by up to 80% of the loaded drug and shortened the implantation process to under one minute. According to *in vitro* release experiments, the distribution of amphotericin B from the drug-loaded PLGA tips takes a week. Antifungal testing on the amphotericin B-loaded PLGA tips demonstrated their effectiveness against *Candida albicans*. For cutaneous fungal infections, the hybrid PLGA-tipped MN system will be appropriate for quick insertion and continuous release of amphotericin B.[91]

There is still a significant international public health concern surrounding the human immunodeficiency virus (HIV).[92] Current antiretroviral (ARV) treatments are taken orally daily, typically for the rest of one's life, resulting in pill fatigue and weak treatment adherence.[93,94] Paredes *et al.* produced dissolving and injectable PLGA MNs loaded with tenofovir alafenamide (TAF). *In vitro* drug release studies on dialysis membrane models revealed that the medication was delivered relatively quickly in all situations. According to Franz cell studies, after 24 hours, dissolving and implantable MNs deposited 47.87 μg and 1208.04 μg of TAF into the skin, respectively. In rat pharmacokinetic studies, TAF was rapidly metabolized into tenofovir, followed by rapid metabolite clearance from the plasma.[95]

4.2.4. Hormonal drug delivery by PLGA-based MNs. Despite significant progress in contraceptive technologies, in 2012, there were 85 million unwanted pregnancies, accounting for 40% of all pregnancies globally.[96] There are 56 million abortions every year to terminate pregnancies.[97] The high rate of unwanted pregnancies burdens women and society financially and emotionally. The absence of contraceptive techniques that broad populations of women can use at different

points in their reproductive life cycle is a major contributor to unwanted pregnancies.[98] Using a controlled casting-mold approach, a new long-acting injectable MN was created to entrap etonogestrel (ENG), third-generation progesterone, in biodegradable PLGA needle tips. MNs were created with high biocompatibility and safety by employing *N*-methyl pyrrolidinone as a solvent for the needle tip matrix. In needle tips, ENG may crystallize evenly. The drug loading capacity of MN formulations was increased to 153.0 μg, and the drug utilization rate was increased to 92.6%. A pharmacokinetic investigation of implanted MNs in rats revealed that the plasma ENG level could be detected for 336 h and that the AUC0-48 h accounted for only 37.8% of the AUC0.[45]

PLGA implantable MNs comprised of PLGA arrowheads encasing levonorgestrel (LNG) and a water-soluble supporting array was developed by Zhao *et al.* The effect of trehalose as a porogen on the release of hydrophobic LNG from PLGA-based MNs was investigated (Fig. 10(a)). During 21 days *in vitro*, the maximum cumulative release of LNG was 76.2% for MNs containing 33.3% trehalose. LNG plasma levels were sustained for 13 days using MNs containing 33.3% trehalose and 16 days using MNs without trehalose. Additionally, PLGA arrowhead MNs with trehalose degraded more quickly than those without trehalose after 21 days. As a result, utilizing trehalose as a porogen to control the release of a hydrophobic medication from PLGA-based MNs seems like a viable option.[27]

Furthermore, Li *et al.* developed a MN patch for the extended release of a contraceptive hormone by entrapping LNG in biodegradable polymer MNs (PLGA and PLA). The air bubble between the MNs and patch support was incorporated into the design to enable quick and easy separation of the MNs from the support upon insertion into the skin. The patch is then removed and discarded as non-sharps waste, which should promote good patient compliance through self-administration. The detached MNs undergo slow biodegradation in the skin for the systemic distribution of encapsulated LNG for more than a month.[98] Another study presented a similar design of separable MNs, including an effervescent backing layer. Sodium bicarbonate and citric acid were used in the MN patch backing as an effervescent combination, which reacted to produce carbon dioxide bubbles upon contact with interstitial fluid in the skin. The method weakened MN adhesion to the patch and allowed detachment within 1 minute after skin insertion. Also, the PLGA matrix containing LNG provided the same sustained release profile over one month. Fig. 10(b) schematically demonstrates this process and provides a plot of the LNG concentration.[99]

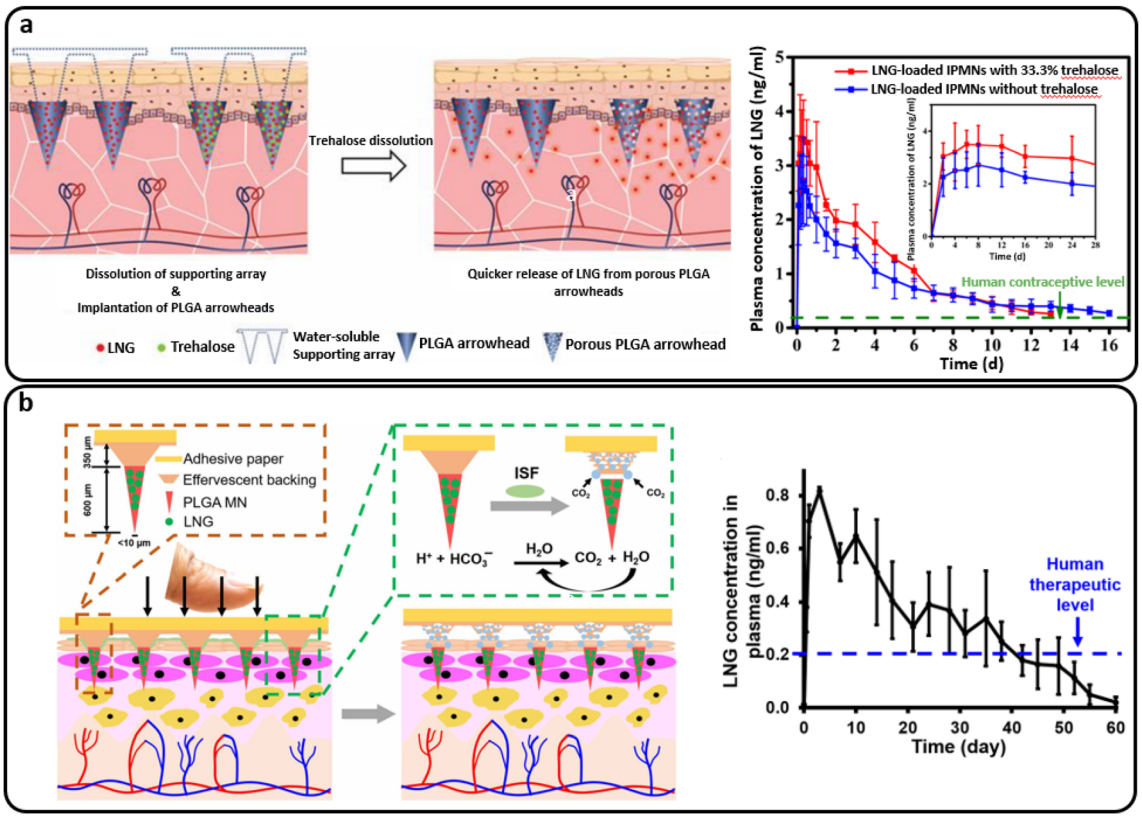

Fig. 10 (a) The intradermal delivery of levonorgestrel (LNG) by PLGA MNs containing trehalose that supplied more than two weeks of human contraceptive level. Reproduced from ref. 27 with permission from MDPI, copyright 2020; (b) a separable PLGA-based MN platform for transdermal LNG delivery that provided a human therapeutic LNG level for over a month. Reproduced from ref. 99 with permission from AAAS, copyright 2019.

In another study, a PLGA MN patch with a PVP porous backing was designed for the extended release of the LNG hormone into the skin as a contraceptive agent. Mechanical strength was maintained during compression to enable MN insertion into the skin, while the porous structure in the patch backing was engineered to reduce the MN interfacial interaction, allowing for simple separation under tension. The MNs prepared from biodegradable PLGA of various molecular weights sustained LNG release from a few days to over one month.[100]

In another study, thermally stable MNs loaded with LNG were created to simplify the preservation and use of PLGA-based MNs in hot seasons and locales. Hydroxypropyl methylcellulose (HPMC) was added to the PLGA-based MNs to boost thermostability due to its superior biocompatibility and high glass transition temperature (T_g). At high temperatures, MNs containing HPMC showed good thermostability. The backing layer of the MNs was degraded *via* interaction with the interstitial fluid of the skin 10 minutes after application, resulting in the separation of the MN tips from the backing layer. The MN tips were inserted intradermally, and the LNG was given through long-term release. The LNG was encapsulated in biodegradable polymers for long-acting prevention. Within 21 days, the *in vitro* release rate of LNG from MNs reached 72.78%–83.76%. In addition, the MNs maintained LNG plasma levels above the human contraceptive threshold in rats for 8–12 days. It took 12–16 days for the inserted MN tips to completely degrade in mice.[101]

Than *et al.* employed PLGA polymers to make MN tips and HA as a sacrificial layer for MN separation. A two-step microforming process was used to load the thyroid hormone T3 and the β3-adrenergic receptor agonist into the PLGA tip MNs. The drug was released once the PLGA slowly biodegraded after the drug-loaded MN tips were inserted into the skin. The MNs quickly detached within 2 minutes due to the quickly dissolving sacrificial layer. These findings demonstrate the promising efficacy of rapidly separable MN patches for treating obesity, showing that slowly degraded MNs released the 3 adrenergic receptor agonist. This method could promote the browning of white adipose tissue and inhibit the increase of body fat and weight in obese mice.[102]

4.2.5. Delivery of other therapeutic agents by PLGA-based MNs. The focus of drug pain therapy is based on opioid receptor agonists.[103] The conventional delivery methods for these medications have considerable health hazards including misuse, addiction, respiratory depression and mortality.[104] These dangers can be reduced by releasing opioids in therapeutic amounts over long periods. Kovaliov *et al.* developed the extended release of synthesized opioid fentanyl analogs by using dissolving MNs and integrating nanoparticles at their tips. Biocompatible fentanyl-bearing polylactide and polyglycolide nanoparticles (Fen-PLA/PLGA nanoparticles) were synthesized using opioid initiators Fen-OH and Fen-Ary-EtOH to generate opioid chain-end functional biodegradable polymers (Fig. 11(a)). In a mouse model of acute nociception, a single subcutaneous dosage of the produced nanoparticles displayed therapeutically appropriate doses for up to six days without undesired burst-release.[105]

Combination therapy is commonly used to treat hypertension since it is low-dose and has fewer negative impacts, such as pretibial edema and gastrointestinal hemorrhage. Sardesai and Shende's study aimed to establish a bio-responsive MN-based enhanced drug delivery system that combined nifedipine (a cardio depressant) and diltiazem (a vasodilator) for successful synergism in the treatment of hypertension. Diltiazem's pH-responsive PLGA nanospheres were produced and mixed with a nifedipine-PVP mixture before being put into a mold to create MNs. Because of the high PVP solubilization, the MNs released about 96.93% of the nifedipine over 24 hours. When diltiazem nanospheres came into contact with the skin's acidic pH, they managed to produce CO_2 bubbles and increase internal pressure, causing the PLGA shell to collapse owing to pore creation. Compared to the disease control group, therapy with this novel composition dramatically decreased the mean blood pressure to 84.11 mmHg (109.9 mmHg). This system co-delivered nifedipine and diltiazem medicines for hypertension, demonstrating an advanced alternative to the traditional drug delivery method.[106]

Finasteride (FND) is a negative regulator of 5-reductase, an enzyme causing benign prostatic hyperplasia (BPH) and androgenic alopecia. FND is generally an oral therapy that lasts a lifetime, adding to the pill load of polymedicated patients.[107] A study by Paredes *et al.* reported soluble and injectable PLGA MNs with the two-week systemic release of FND (Fig. 11(b)). *In vitro* tests showed that the dissolving and implantable MNs could release the medication for up to seven and 14 days, respectively. In Franz cells, skin deposition studies revealed that dissolving and implantable MNs could deposit 629 μg and 1861.64 μg of FND, respectively, after 24 hours. On the other hand, transdermal penetration tests showed that both formulations released the drug slowly to the receptor compartment of the Franz cells, with dissolving and injectable MNs releasing 90.43 μg and 27.80 μg of FND after 24 hours, respectively. The combinations presented here might be an alternative to conventional oral therapies for BPH and androgenic alopecia.[108]

Mesenchymal stem cells (MSCs), extensively employed for regenerative therapy, are injected in most current clinical applications. Due to the MSC's low capability for migration, it has severe challenges with cell viability and penetration into the target tissue. By encapsulating MSCs in biomaterials, several therapies have been used to try to increase their stability; nevertheless, owing to their poor efficiency, these therapies still need many cells to be therapeutically effective. Furthermore, whereas local injection enables tailored administration, typical syringe injections are inherently invasive. Due to the difficulties of delivering stem cells, it is extremely desirable to use a localized, minimally invasive method that is highly effective and improves cell survival. Lee *et al.* investigated a detachable hybrid MN depot for MSC delivery. As shown in Fig. 11(c), the device was composed of an array of MNs with an outer PLGA shell and an internal gelatin metha-

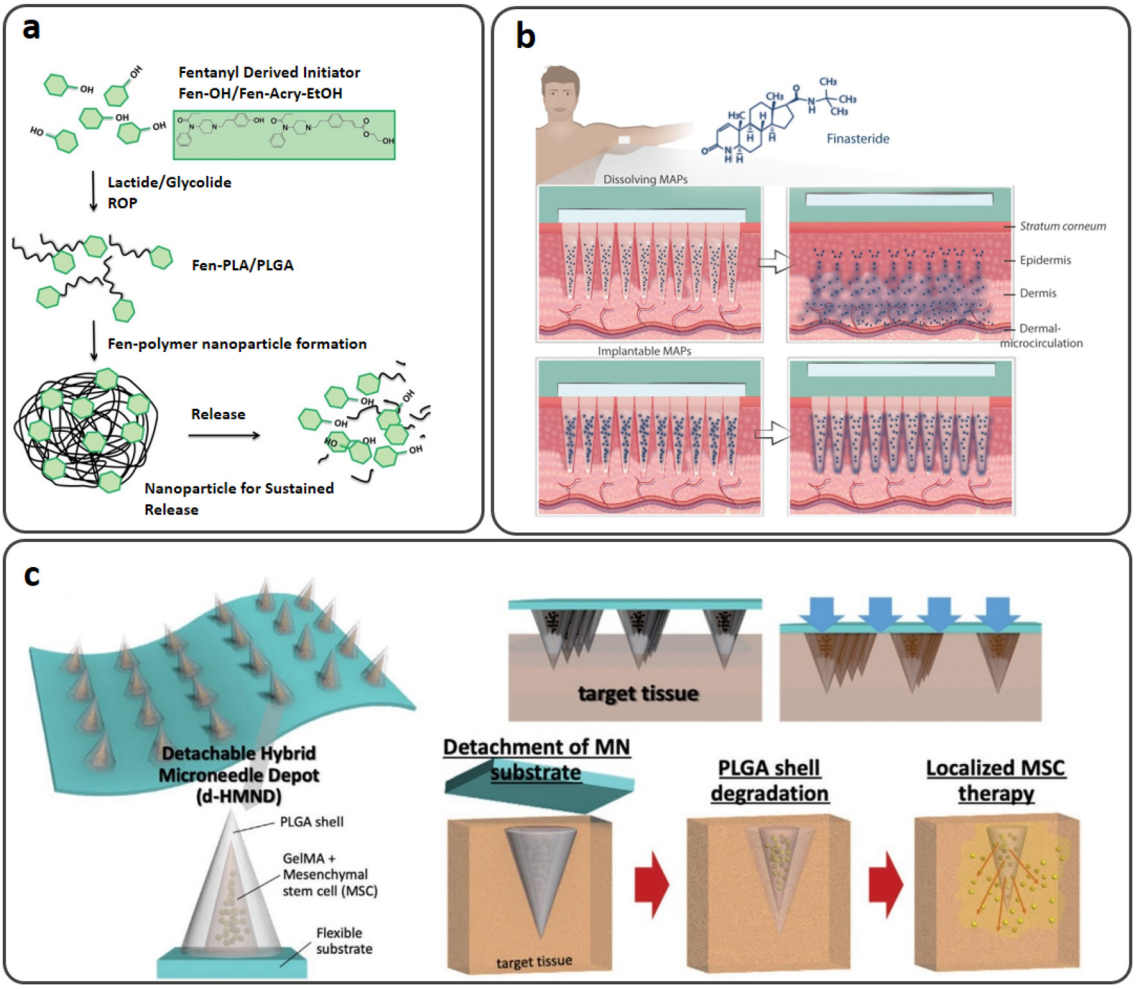

Fig. 11 (a) Biocompatible fentanyl (Fen)-bearing PLA/PLGA nanoparticle-based dissolvable MNs. Reproduced from ref. 105 with permission from RSC, copyright 2017; (b) injectable PLGA MNs for intradermal release of finasteride (FND). Reproduced from ref. 108 with permission from Elsevier, copyright 2021; (c) a d-HMND constructed from a GelMA–MSC mixture loaded in PLGA shells attached to a flexible substrate and the delivery mechanism. Reproduced from ref. 109 with permission from Wiley, copyright 2020.

cryloyl (GelMA)–MSC mixture (GMM), which was designed as a detachable hybrid MN depot (d-HMND). A two-step molding procedure with plasma surface modification was used to create the PLGA shell. A GMM with a 30 kPa compressive modulus for MSC viability was evaluated and optimized. The PLGA shells were filled with GMM, and the array of MNs displayed high mechanical integrity and sufficient strength to penetrate the target tissue. Wound closure, re-epithelialization, and CD31-positive microvasculature were all improved in d-HMND-treated animals compared to controls. A novel cell therapy delivery technology, such as d-HMND, may enhance the treatment of skin wounds by using MSCs.[109]

Ullah *et al.* demonstrated that MNs coated with a porous PLGA polymer were capable of high-rate drug delivery. To improve delivery rates, stainless steel MNs with high mechanical strength were covered with a thin porous polymer coating. Furthermore, the MN surface was changed by plasma treatment followed by dip coating with PEI to increase interfacial adhesion between the polymer and MNs. The permeable polymer-coated MNs efficiently transported calcein dye into pig skin to a depth of 750 μm. RhB and lidocaine were administered deeply *via* porous-coated MNs compared to non-coated MNs in a gelatin gel.[110] In another similar formulation, the PLGA porous-coated MNs effectively transported calcein dye into pig skin to a depth of 750 μm. Furthermore, porous-coated MNs delivered 25 times more lidocaine than non-coated MNs.[111]

The various PLGA-based MNs for the intradermal delivery of drugs and therapeutic agents are introduced in Table 3.

4.3. Vitamin and protein/enzyme delivery

4.3.1. Protein/enzyme delivery by PLGA-based MNs. Proteins are extensively investigated as bioactive molecules, but some problems include remaining intact for their delivery to targeted tissues and organs.[3] If not adequately stored or after they have come into contact with the biological environ-

ment, water-labile proteins, in particular, are prone to quick failure. Delivery methods can particularly protect such proteins during storage and delivery.[112] Polymer MNs are promising tools for delivering proteins *in vivo* while avoiding harsh gastrointestinal and blood environments.[3] Table 4 summarizes the performance of PLGA-based MNs for protein/enzyme delivery.

In a study by Park *et al.*, layered MNs were manufactured by spraying PLGA and PVP in order, and their *ex vivo* skin penetration tests were described (Fig. 12(a)). The MNs were injected into the skin, and histological investigation showed the biphasic release of colors inside the MN matrices. The findings revealed that the tertiary structure of BSA was preserved in both the PLGA and PVP layers, whereas the secondary structures were minimally altered during the manufacture of MNs. *In vitro* release investigations revealed that over 60% of the BSA in the PLGA layer was released within an hour, with continued slow release throughout the trial (seven days).[113]

Table 4 PLGA-based MN delivery of proteins and vitamins

Delivery agents	Type of MNs	Design strategy	Drug/therapeutic agents	Animal skin model	Ref.
Proteins/ Enzymes	Dissolving MNs	Spraying PLGA and PVP on layered MNs	BSA	Porcine	113
		Enzyme-loaded PLGA MNs	POXA1b laccase	Porcine	114
		PVP-hyaluronic acid (PVP-HA) integrated PLGA microparticles	Collagenase	Rats	115
		PVP, HA, and PLGA-based MNs	Lysozyme	Rats	116
		OVA-encapsulated PLGA MNs	Ovalbumin (OVA)	Porcine	118
	Coated MNs	OVA-loaded PLGA/hydrogel MN		Mice	117
Vitamins	Dissolving MNs	Niacinamide/PLGA gel MNs	Niacinamide (VB3)	Porcine	121
		VD3-loaded PLGA nanoparticles and microparticles	Vitamin D3 (VD3)	Porcine	26
	Solid MNs	VD3-loaded PLGA MNs			119

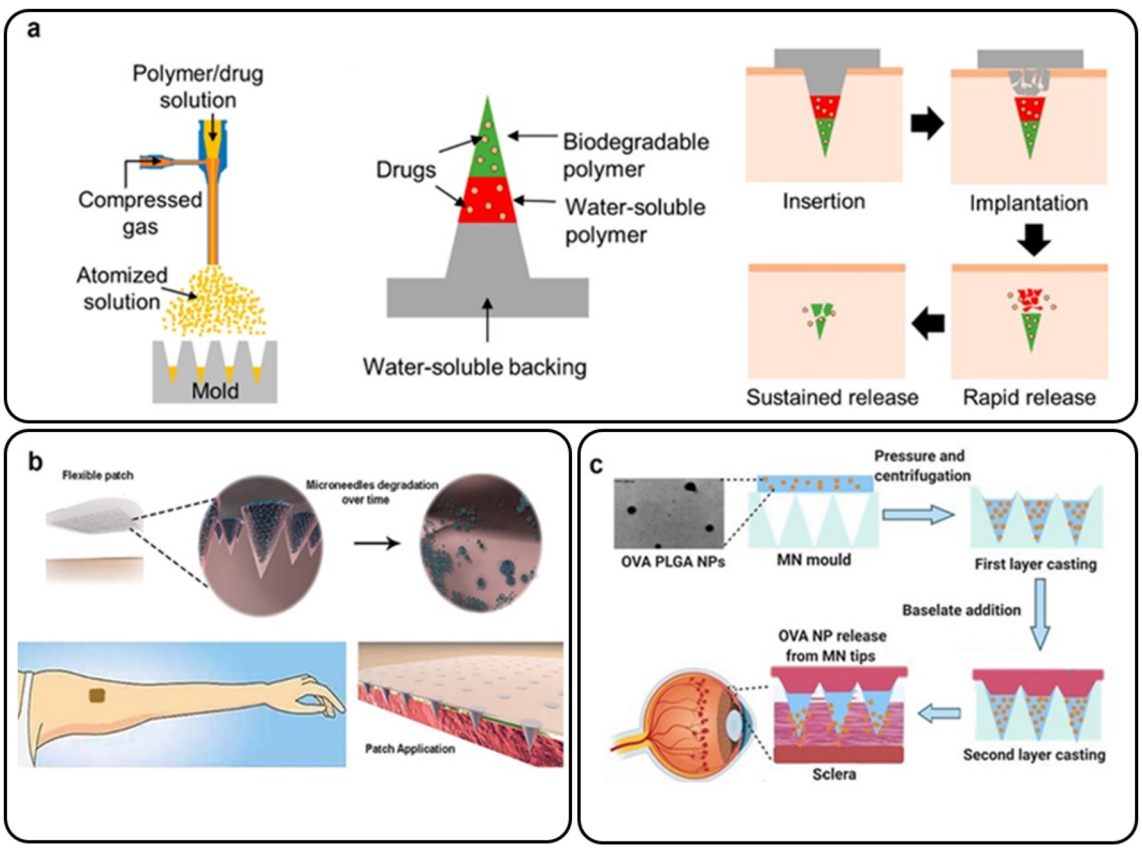

Fig. 12 (a) Layered PLGA/PVP MNs for the transdermal delivery of BSA. Reproduced from ref. 113 with permission from MDPI, copyright 2019; (b) an array of MNs containing biodegradable PLGA microparticles for intradermal delivery of POXA1b laccase. Reproduced from ref. 114 with permission from Frontiers Media S.A., copyright 2019; (c) bilayer OVA-encapsulated PLGA nanoparticle-based MN arrays. Reproduced from ref. 118 with permission from Elsevier, copyright 2021.

A unique stamp-based MN manufacturing approach was suggested by Battisti *et al.* that involved the quick room-temperature synthesis of multi-compartmental biodegradable polymeric MNs for regulated intradermal enzyme release. An array of MNs with configurable delivery was created using PVP-based short solubilized tips and biodegradable PLGA MNs. Pig cadaver skin was used to examine the ability of the resultant MNs to penetrate it. POXA1b laccase as a model medicine was loaded into both the tip and the body of the MNs. POXA1b laccase from *Pleurotus ostreatus* is a commercial enzyme used to whiten skin patches (Fig. 12(b)). In an *in vitro* skin model, the enzyme-loaded MN activities were evaluated, highlighting their potential to regulate the kinetic release of the encapsulated chemical.[114]

Polymer MNs were provided for the packaging and transporting of the fragile protein collagenase. PVP–hyaluronic acid (PVP-HA) MNs with integrated PLGA MNs were created to provide a continuous yet quick release of the enzyme, avoiding prolonged exposure to water after delivery. A modified double emulsion process was used to create PLGA microparticles with variable permeability. The suggested release and compaction capabilities of microparticle-based MNs were confirmed using diffusion tests and *in vivo* trials.[115]

Polymeric MNs were employed by Panda *et al.* to entrap lysozyme (14 kDa) utilizing biodegradable polymers including PVP, HA and PLGA. A mold-casting process was used to create the MNs. In the cases of PVP and HA, approximately half of the drug was released within the first 20 minutes in both cases, and the rest was released during the following 2 hours. In contrast, lysozyme entrapped in PLGA revealed a release of 29.53 ± 0.78% of lysozyme at 72 hours. For PVP, HA and PLGA, the lysozyme concentration captured at the end of 90 days was 90.35%, 93.76%, and 91.74%, respectively. The protein integrity in the three polymeric MNs was preserved for three months. According to the enzyme analysis, the enzyme entrapped inside the MNs was physiologically active and might be utilized to treat wounds and skin infections.[116]

The use of electrohydrodynamic atomization (EHDA) to coat OVA-loaded PLGA nanoparticles onto hydrogel-forming MN arrays was described by Angkawinitwong *et al.* Over 28 days, the particles continued to release OVA. *In vivo*, the covered MNs did not cause a significant rise in anti-OVA-specific IgG titers in C57BL/6 mice, demonstrating that the formulations were unrelated to immunogenicity. As a result, coating a MN array with EHDA appears to hold promise as a new non-invasive protein delivery mechanism.[117]

Wu *et al.* prepared nanoparticle-loaded bilayer dispersing MN arrays using OVA-encapsulated PLGA nanoparticles as a template protein (Fig. 11(c)). The decreased main sonication duration could sustain release (77 days at 28.5% OVA loading) and boost OVA bioactivity. The adjusted nanoparticles were then integrated into a polymeric matrix to generate bilayer MNs, and high-speed centrifugation was used to condense the nanoparticles into MN tips. In excised porcine sclera, optimized bilayer MNs showed good mechanical and insertion capabilities and quick dissolving kinetics (less than three minutes). *Ex vivo* transscleral dispersion experiments verified the critical role of MN arrays in the localization of proteins and nanoparticles in scleral tissue. Moreover, it was shown that the polymers used to make bilayer MNs and OVA nanoparticles were biocompatible with retinal cells (ARPE-19). This method of administration might enable encapsulated proteins to be released for up to two months and efficiently circumvent the scleral barrier, making it a viable treatment for neovascular ocular disorders.[118]

4.3.2. Vitamin delivery by PLGA-based MNs. Since vitamin D3 (VD3), the most common form of vitamin D, can be generated in human skin when exposed to sunshine, vitamin D insufficiency has become a serious international public health concern.[119,120] Oral supplements or vitamin D-fortified meals are commonly given to aid vitamin D consumption. Oral techniques are rare in certain areas, and oral absorption is inefficient due to numerous obstacles and varying environmental conditions. Furthermore, vitamin D should be taken daily to sustain a sufficient level in the blood. Instead, because of its benefits, such as eliminating the liver's first-pass impact and allowing for long-term release, a transdermal delivery method might provide a practical approach to acquiring a prolonged dosage of vitamin D.

For targeted and maintained intradermal drug administration, Vora *et al.* created biodegradable bilayer MN arrays containing VD3-loaded PLGA nanoparticles and microparticles with 72.8% VD3 (Fig. 13). The particle size of PLGA varied from 300 nm to 3.5 μm. It remained the same when bilayer MN arrays were molded. The PLGA particle drug dissolution characteristic was tri-phasic and lasted for five days. After cryostatic skin segmentation, *ex vivo* intradermal neonatal pig skin penetration of VD3 particles from bilayer MNs was quantified, with 74.2% of VD3 loading being delivered intradermally. The proposed quick and straightforward approach for localizing particle delivery systems into dissolving MNs was a two-stage unique processing procedure.[26]

Kim *et al.* developed a transdermal delivery mechanism for prolonged vitamin D release by employing coated MNs that could also readily penetrate the skin layer. VD3-entrapped PLGA showed adequate qualities for transdermal administration such as size distribution, skin tolerance and efficient release of the encapsulated chemical. Finally, PVD3 layers coated on solid MNs were entirely dissolved in the intradermal area of a pig skin model, demonstrating greater VD3 release into plasma than the ointment-based transdermal approach.[119]

Work by Bhattaccharjee *et al.* aimed to take advantage of PLGA's capacity to gel *in situ* and improve the topical administration of niacinamide (a type of vitamin B3) to microporated skin. *In vitro* drug penetration tests were conducted using vertical Franz diffusion cells. Upon application to microporated skin, PLGA-containing formulations gelled well *in situ*. With 0.5 mm treatment for 5 seconds, different grades of PLGA revealed considerably larger quantities of medication in the skin. This rate was more significant for the higher molecular weight polymer than for the lower molecular weight

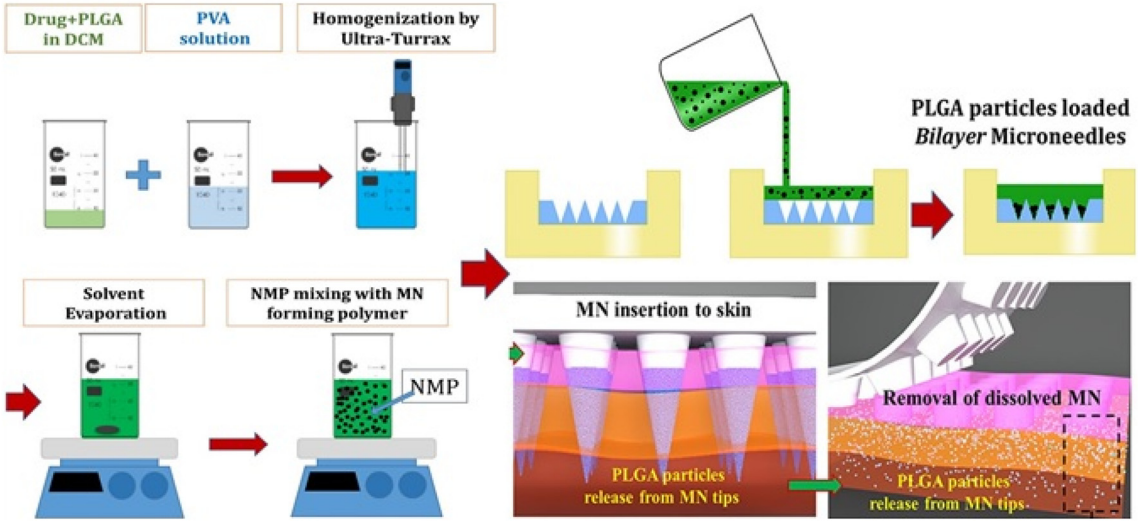

Fig. 13 Dissolvable bilayer MN arrays containing VD3-loaded PLGA nanoparticles and microparticles. Reproduced from ref. 26 with permission from Elsevier, copyright 2017.

polymer.[121] Reported intradermal vitamin delivery by PLGA-based MNs is summarized in Table 4.

5. Conclusions and future perspectives

Over the last few years, MNs have attracted much interest from the medical, biological, disease treatment and pharmaceutical areas.[122,123] Polymeric MNs, in particular, provide a drug delivery system with better local drug permeation and bioavailability. These advantages enable them to be used in various medication delivery systems.[124] According to studies, PLGA with strong biocompatibility and biodegradability has attracted a lot of interest. PLGA is a nontoxic polymer. As a result of these events, PLGA-based MNs are being used. PLGA-based MNs have been utilized to deliver various medications effectively. These techniques, however, are still in their infancy. Future possibilities for PLGA-based MNs include adding targeting units, such as aptamers or peptides, to improve delivery to local sites; optimizing therapeutic drug concentrations; and including penetration-enhancing compounds in their formulations. The drug loaded into PLGA MNs electrostatically engages with negatively charged receptors on tissues or cells thanks to the positive charge of PLGA. It was shown that PLGA MNs could aid in the opening of tight intersections. It takes a long time for medications wrapped in PLGA-based MNs to be released entirely. While the PLGA composition is unchanging, it is still important to control the release of medicines from MNs to achieve the appropriate duration.

At this point, there is no information on PLGA-based MNs that can be widely used in the clinic. Given the advancement of nanotechnology in clinical applications, PLGA-based MNs can be endorsed as future beneficial innovative systems for drug delivery. Biodegradable and dissolved PLGA-based MNs, unlike non-biodegradable forms, vanish from the administration site after delivering the medicine. Moreover, it seems the injection of dissolvable MNs made from PLGA is well tolerated in animals and humans. Biodegradable MNs might even help improve regenerative medicine in the future.

Conflicts of interest

There are no conflicts to declare.

References

1 L. K. Vora, K. Moffatt, I. A. Tekko, A. J. Paredes, F. Volpe-Zanutto, D. Mishra, K. Peng, R. Raj Singh Thakur and R. F. Donnelly, *Eur. J. Pharm. Biopharm.*, 2021, **159**, 44–76.
2 J. Yang, X. Liu, Y. Fu and Y. Song, *Acta Pharm. Sin. B*, 2019, **9**, 469–483.
3 R. Jamaledin, C. Di Natale, V. Onesto, Z. B. Taraghdari, E. N. Zare, P. Makvandi, R. Vecchione and P. A. Netti, *J. Clin. Med.*, 2020, **9**, 542.
4 L. Dsouza, V. M. Ghate and S. A. Lewis, *Biomed. Microdevices*, 2020, **22**, 1–11.
5 K. A. S. Al-japairai, S. Mahmood, S. H. Almurisi, J. Reddy, A. Rebhi, M. Azmana and S. Raman, *Int. J. Pharm.*, 2020, **587**, 119673.
6 Z. Sartawi, C. Blackshields and W. Faisal, *J. Controlled Release*, 2022, **348**, 186–205.
7 I. Menon, P. Bagwe, K. B. Gomes, L. Bajaj, R. Gala, M. N. Uddin, M. J. D'souza and S. M. Zughaier, *Micromachines*, 2021, **12**, 1–18.
8 K. van der Maaden, W. Jiskoot and J. Bouwstra, *J. Controlled Release*, 2012, **161**, 645–655.

9 A. J. Guillot, A. S. Cordeiro, R. F. Donnelly, M. C. Montesinos, T. M. Garrigues and A. Melero, *Pharmaceutics*, 2020, **12**, 1–28.
10 E. Larrañeta, R. E. M. Lutton, A. D. Woolfson and R. F. Donnelly, *Mater. Sci. Eng., R*, 2016, **104**, 1–32.
11 R. F. Donnelly, T. R. Singh, M. J. Garland, K. Migalska, R. Majithiya, C. M. McCrudden, P. L. Kole, T. M. Mahmood, H. O. McCarthy and A. D. Woolfson, *Adv. Funct. Mater.*, 2012, **22**, 4879–4890.
12 J. G. Turner, L. R. White, P. Estrela and H. S. Leese, *Macromol. Biosci.*, 2021, **21**, 2000307.
13 A. J. Courtenay, E. McAlister, M. T. C. McCrudden, L. Vora, L. Steiner, G. Levin, E. Levy-Nissenbaum, N. Shterman, M.-C. Kearney, H. O. McCarthy and R. F. Donnelly, *J. Controlled Release*, 2020, **322**, 177–186.
14 P. Serrano-Castañeda, J. J. Escobar-Chavez, I. M. Rodriguez-Cruz, L. M. Melgoza and J. Martinez-Hernandez, *J. Pharm. Pharm. Sci.*, 2018, **21**, 73–93.
15 K. Lavanya, S. V. Chandran, K. Balagangadharan and N. Selvamurugan, *Mater. Sci. Eng., C*, 2020, **111**, 110862.
16 X. Meng, Z. Zhang and L. Li, *Prog. Nat. Sci.: Mater. Int.*, 2020, **30**, 589–596.
17 B. Begines, T. Ortiz, M. Pérez-Aranda, G. Martínez, M. Merinero, F. Argüelles-Arias and A. Alcudia, *Nanomaterials*, 2020, **10**, 1403.
18 K. Zhi, B. Raji, A. R. Nookala, M. M. Khan, X. H. Nguyen, S. Sakshi, T. Pourmotabbed, M. M. Yallapu, H. Kochat, E. Tadrous, S. Pernell and S. Kumar, *Pharmaceutics*, 2021, **13**, 500.
19 S. R. Pardeshi, A. Nikam, P. Chandak, V. Mandale, J. B. Naik and P. S. Giram, *Int. J. Polym. Mater. Polym. Biomater.*, 2023, **72**, 49–78.
20 C. Dwivedi, I. Pandey, H. Pandey, P. W. Ramteke, A. C. Pandey, S. B. Mishra and S. Patil, in *Electrospun Nanofibrous Scaffold as a Potential Carrier of Antimicrobial Therapeutics for Diabetic Wound Healing and Tissue Regeneration*, ed. A. M. B. T.-N. M. D. D. S. Grumezescu, Elsevier, 2017, ch. 9, pp. 147–164.
21 A. Cunha, A. Gaubert, L. Latxague and B. Dehay, *Pharmaceutics*, 2021, **13**, 1042.
22 S. Mansoor, P. P. D. Kondiah, Y. E. Choonara and V. Pillay, *Polymers*, 2019, **11**, 1380.
23 E. Lagreca, V. Onesto, C. Di Natale, S. La Manna, P. A. Netti and R. Vecchione, *Prog. Biomater.*, 2020, **9**, 153–174.
24 A. Kumari, S. K. Yadav and S. C. Yadav, *Colloids Surf., B*, 2010, **75**, 1–18.
25 S. M. Kim, M. Patel and R. Patel, *Polymers*, 2021, **13**, 3471.
26 L. K. Vora, R. F. Donnelly, E. Larrañeta, P. González-Vázquez, R. R. S. Thakur and P. R. Vavia, *J. Controlled Release*, 2017, **265**, 93–101.
27 X. Zhao, S. Zhang, G. Yang, Z. Zhou and Y. Gao, *Polymers*, 2020, **12**, 59.
28 H. Li, Z. Wang, E. A. Ogunnaike, Q. Wu, G. Chen, Q. Hu, T. Ci, Z. Chen, J. Wang, D. Wen, H. Du, J. Jiang, J. Sun, X. Zhang, G. Dotti and Z. Gu, *Natl. Sci. Rev.*, 2021, **9**, 172.
29 M. A. Washington, S. C. Balmert, M. V. Fedorchak, S. R. Little, S. C. Watkins and T. Y. Meyer, *Acta Biomater.*, 2018, **65**, 259–271.
30 T. A. Mehta, N. Shah, K. Parekh, N. Dhas and J. K. Patel, *Surface-Modified PLGA Nanoparticles for Targeted Drug Delivery to Neurons*, 2019.
31 L. Del Amo, A. Cano, M. Ettcheto, E. B. Souto, M. Espina, A. Camins, M. L. García and E. Sánchez-López, *Appl. Sci.*, 2021, **11**, 4305.
32 H. K. Makadia and S. J. Siegel, *Polymers*, 2011, **3**, 1377–1397.
33 Y. Morishita, N. Takama and B. Kim, in *2018 IEEE CPMT Symposium Japan (ICSJ)*, 2018, pp. 81–84.
34 A. Butreddy, R. P. Gaddam, N. Kommineni, N. Dudhipala and C. Voshavar, *Int. J. Mol. Sci.*, 2021, **22**, 8884.
35 A. Malek-Khatabi, Z. Faraji Rad, M. Rad-Malekshahi and H. Akbarijavar, *Mater. Lett.*, 2023, **330**, 133328.
36 J.-H. Park, S.-O. Choi, R. Kamath, Y.-K. Yoon, M. G. Allen and M. R. Prausnitz, *Biomed. Microdevices*, 2007, **9**, 223–234.
37 K. T. Tu and C. K. Chung, *J. Micromech. Microeng.*, 2016, **26**, 65015.
38 F. Ruggiero, R. Vecchione, S. Bhowmick, G. Coppola, S. Coppola, E. Esposito, V. Lettera, P. Ferraro and P. A. Netti, *Sens. Actuators, B*, 2018, **255**, 1553–1560.
39 V. Onesto, C. Di Natale, M. Profeta, P. A. Netti and R. Vecchione, *Prog. Biomater.*, 2020, **9**, 203–217.
40 H. Lim, S. Ha, M. Bae and S.-H. Yoon, *Int. J. Pharm.*, 2021, **600**, 120475.
41 Q. Tian, H. N. Chan, Y. Chen and H. Wu, MicroTAS 2015 – 19th Int. Conf. Miniaturized Syst. Chem. Life Sci., 2015, 1, 1469–1471.
42 M. J. Kim, S. C. Park and S.-O. Choi, *RSC Adv.*, 2017, **7**, 55350–55359.
43 Y.-C. Huang, P.-W. Lin, W.-J. Qiu and T.-I. Yang, *Biomed. Eng. Appl. Basis Commun.*, 2016, **28**, 1650013.
44 A. Panda, P. K. Sharma, T. McCann, J. Bloomekatz, M. A. Repka and S. N. Murthy, *J. Drug Delivery Sci. Technol.*, 2022, **68**, 102712.
45 M. He, G. Yang, X. Zhao, S. Zhang and Y. Gao, *J. Pharm. Sci.*, 2020, **109**, 1958–1966.
46 J. Lee, S. H. Park, E. H. Jang, J. H. Kim, Y. N. Youn and W. Ryu, Fabrication and characterization of silk fibroin microneedle meshes for perivascular drug delivery, In Society for Biomaterials Annual Meeting and Exposition 2019, The Pinnacle of Biomaterials Innovation and Excellence - Transactions of the 42nd Annual Meeting, *Trans. Annu. Meet. Soc. Biomater. Annu. Int. Biomater. Symp.*, 2019, vol. **40**, p. 68.
47 S. Zhang, W. Gao, J. Zhu, Q. G. Zhang, M. Wang and X. Y. Gao, *Acad. J. Second Mil. Med. Univ.*, 2010, **12**, 1341–1345.
48 W. Zhang, B. Ding, R. Tang, X. Ding, X. Hou, X. Wang, S. Gu, L. Lu, Y. Zhang, S. Gao and J. Gao, *Curr. Nanosci.*, 2011, **7**, 545–551.

49 R. F. Donnelly, D. I. J. Morrow, F. Fay, C. J. Scott, S. Abdelghany, R. R. T. Singh, M. J. Garland and A. D. Woolfson, *Photodiagn. Photodyn. Ther.*, 2010, **7**, 222–231.
50 Y. A. Gomaa, L. K. El-Khordagui, M. J. Garland, R. F. Donnelly, F. McInnes and V. M. Meidan, *J. Pharm. Pharmacol.*, 2012, **64**, 1592–1602.
51 Y. A. Gomaa, M. J. Garland, F. J. McInnes, R. F. Donnelly, L. K. El-Khordagui and C. G. Wilson, *Eur. J. Pharm. Biopharm.*, 2014, **86**, 145–155.
52 C. Lee, J. Kim, D. J. Um, Y. Kim, H. S. Min, J. Shin, J. H. Nam, G. Kang, M. Jang, H. Yang and H. Jung, *Pharmaceutics*, 2021, **13**, 1058.
53 D. C. Pawley, S. Goncalves, E. Bas, E. Dikici, S. K. Deo, S. Daunert and F. Telischi, *Adv. Ther.*, 2021, **4**, 2100155.
54 J. M. Mazzara, M. A. Balagna, M. D. Thouless and S. P. Schwendeman, *J. Controlled Release*, 2013, **171**, 172–177.
55 J. J. Norman, S.-O. Choi, N. T. Tong, A. R. Aiyar, S. R. Patel, M. R. Prausnitz and M. G. Allen, *Biomed. Microdevices*, 2013, **15**, 203–210.
56 P. C. Demuth, W. F. Garcia-Beltran, M. L. Ai-Ling, P. T. Hammond and D. J. Irvine, *Adv. Funct. Mater.*, 2013, **23**, 161–172.
57 M. R. Prausnitz, J. A. Mikszta, M. Cormier and A. K. Andrianov, *Curr. Top. Microbiol. Immunol.*, 2009, **333**, 369–393.
58 J. Wallis, D. P. Shenton and R. C. Carlisle, *Clin. Exp. Immunol.*, 2019, **196**, 189–204.
59 A. Malek-Khatabi, Z. Tabandeh, A. Nouri, E. Mozayan, R. Sartorius, S. Rahimi and R. Jamaledin, *ACS Appl. Bio Mater.*, 2022, **11**, 5015–5040.
60 T. Wang and N. Wang, *Curr. Pharm. Des.*, 2015, **21**, 5245–5255.
61 G. Du, R. M. Hathout, M. Nasr, M. R. Nejadnik, J. Tu, R. I. Koning, A. J. Koster, B. Slütter, A. Kros, W. Jiskoot, J. A. Bouwstra and J. Mönkäre, *J. Controlled Release*, 2017, **266**, 109–118.
62 A. M. de Groot, G. Du, J. Mönkäre, A. C. M. Platteel, F. Broere, J. A. Bouwstra and A. J. A. M. Sijts, *J. Controlled Release*, 2017, **266**, 27–35.
63 L. Niu, L. Y. Chu, S. A. Burton, K. J. Hansen and J. Panyam, *J. Controlled Release*, 2019, **294**, 268–278.
64 M. Zaric, O. Lyubomska, O. Touzelet, C. Poux, S. Al-Zahrani, F. Fay, L. Wallace, D. Terhorst, B. Malissen, S. Henri, U. F. Power, C. J. Scott, R. F. Donnelly and A. Kissenpfennig, *ACS Nano*, 2013, **7**, 2042–2055.
65 J. Mönkäre, M. Pontier, E. E. M. van Kampen, G. Du, M. Leone, S. Romeijn, M. R. Nejadnik, C. O'Mahony, B. Slütter, W. Jiskoot and J. A. Bouwstra, *Eur. J. Pharm. Biopharm.*, 2018, **129**, 111–121.
66 H. W. Yang, L. Ye, X. D. Guo, C. Yang, R. W. Compans and M. R. Prausnitz, *Adv. Healthcare Mater.*, 2017, **6**, 1–7.
67 C. Bernelin-Cottet, C. Urien, J. McCaffrey, D. Collins, A. Donadei, D. McDaid, V. Jakob, C. Barnier-Quer, N. Collin, E. Bouguyon, E. Bordet, C. Barc, O. Boulesteix, J.-J. Leplat, F. Blanc, V. Contreras, N. Bertho, A. C. Moore and I. Schwartz-Cornil, *J. Controlled Release*, 2019, **308**, 14–28.
68 S. Shao, O. A. Ortega-Rivera, S. Ray, J. K. Pokorski and N. F. Steinmetz, *Vaccines*, 2021, **9**, 66.
69 K. Braz Gomes, B. D'Souza, S. Vijayanand, I. Menon and M. J. D'Souza, *Int. J. Pharm.*, 2022, **613**, 121393.
70 A. F. Lima, I. R. Amado and L. R. Pires, *Polymers*, 2020, **12**, 3063.
71 M. Waghchaure, S. Govardhane and P. Shende, *Biomed. Microdevices*, 2021, **23**, 32.
72 D. Pushparajah, S. Jimenez, S. Wong, H. Alattas, N. Nafissi and R. A. Slavcev, *Adv. Drug Delivery Rev.*, 2021, **170**, 113–141.
73 M. Pearton, C. Allender, K. Brain, A. Anstey, C. Gateley, N. Wilke, A. Morrissey and J. Birchall, *Pharm. Res.*, 2008, **25**, 407–416.
74 A. Kumar, P. Wonganan, M. A. Sandoval, X. Li, S. Zhu and Z. Cui, *J. Controlled Release*, 2012, **163**, 230–239.
75 H. Seok, J. Y. Noh, D. Y. Lee, S. J. Kim, C. S. Song and Y. C. Kim, *J. Controlled Release*, 2017, **265**, 66–74.
76 Y. Ma, S. E. Boese, Z. Luo, N. Nitin and H. S. Gill, *Biomed. Microdevices*, 2015, **17**, 44.
77 C. Kwak, S. E. Lee, I. G. Jeong and J. H. Ku, *Urology*, 2006, **68**, 53–57.
78 W. Hohenforst-Schmidt, P. Zarogoulidis, K. Darwiche, T. Vogl, E. P. Goldberg, H. Huang, M. Simoff, Q. Li, R. Browning, F. J. Turner, P. Le Pivert, D. Spyratos, K. Zarogoulidis, S. I. Celikoglu, F. Celikoglu and J. Brachmann, *Drug Des., Dev. Ther.*, 2013, **7**, 571–583.
79 M. S. Razavi, A. Abdollahi, A. Malek-Khatabi, N. M. Ejarestaghi, A. Atashi, N. Yousefi, P. Ebrahimnejad, M. A. Elsawy and R. Dinarvand, *J. Drug Delivery Sci. Technol.*, 2023, **85**, 104587.
80 A. H. Sabri, Y. Kim, M. Marlow, D. J. Scurr, J. Segal, A. K. Banga, L. Kagan and J. B. Lee, *Adv. Drug Delivery Rev.*, 2020, **153**, 195–215.
81 M. Ibrahim, W. H. Abuwatfa, N. S. Awad, R. Sabouni and G. A. Husseini, *Pharmaceutics*, 2022, **14**, 254.
82 B. Carrese, C. Cavallini, G. Sanità, P. Armanetti, B. Silvestri, G. Calì, G. Pota, G. Luciani, L. Menichetti and A. Lamberti, *Int. J. Mol. Sci.*, 2021, **22**, 11228.
83 H. X. Nguyen and A. K. Banga, *Pharm. Res.*, 2018, **35**, 68.
84 M. S. Chellathurai, V. W. T. Ling and V. K. Palanirajan, *Turk. J. Pharm. Sci.*, 2021, **18**, 96–103.
85 H. Yang, S. Kim, I. Huh, S. Kim, S. F. Lahiji, M. Kim and H. Jung, *Biomaterials*, 2015, **64**, 70–77.
86 M. Rabiei, S. Kashanian, G. Bahrami, H. Derakhshankhah, E. Barzegari, S. S. Samavati and S. J. P. McInnes, *Eur. J. Pharm. Sci.*, 2021, **167**, 106040.
87 J. Holl, C. Kowalewski, Z. Zimek, P. Fiedor, A. Kaminski, T. Oldak, M. Moniuszko and A. Eljaszewicz, *Cells*, 2021, **10**, 655.
88 Y. Tang, M. J. Zhang, J. Hellmann, M. Kosuri, A. Bhatnagar and M. Spite, *Diabetes*, 2013, **62**, 618–627.

89 L. Long, W. Liu, L. Li, C. Hu, S. He, L. Lu, J. Wang, L. Yang and Y. Wang, *Nanoscale*, 2022, **14**, 1285–1295.
90 R. Jamaledin, C. K. Y. Yiu, E. N. Zare, L.-N. Niu, R. Vecchione, G. Chen, Z. Gu, F. R. Tay and P. Makvandi, *Adv. Mater.*, 2020, **32**, 2002129.
91 K. Peng, L. K. Vora, J. Domínguez-Robles, Y. A. Naser, M. Li, E. Larrañeta and R. F. Donnelly, *Mater. Sci. Eng., C*, 2021, **127**, 112226.
92 M. Saravanan, T. Asmalash, A. Gebrekidan, D. Gebreegziabiher, T. Araya, H. Hilekiros, H. Barabadi and K. Ramanathan, *Pharm. Nanotechnol.*, 2018, **6**, 17–27.
93 M. Vitoria, A. Rangaraj, N. Ford and M. Doherty, *Curr. Opin. HIV AIDS*, 2019, **14**, 143–149.
94 N. Phanuphak and R. M. Gulick, *Curr. Opin. HIV AIDS*, 2020, **15**, 4–12.
95 A. J. Paredes, F. Volpe-Zanutto, L. K. Vora, I. A. Tekko, A. D. Permana, C. J. Picco, H. O. McCarthy and R. F. Donnelly, *Mater. Today Bio*, 2022, **13**, 100217.
96 G. Sedgh, S. Singh and R. Hussain, *Stud. Fam. Plann.*, 2014, **45**, 301–314.
97 S. Singh *et al.*, *Abortion Worldwide 2017: Uneven Progress and Unequal Access*, Guttmacher Institute, New York, 2018.
98 W. Li, R. N. Terry, J. Tang, M. R. Feng, S. P. Schwendeman and M. R. Prausnitz, *Nat. Biomed. Eng.*, 2019, **3**, 220–229.
99 W. Li, J. Tang, R. N. Terry, S. Li, A. Brunie, R. L. Callahan, R. K. Noel, C. A. Rodríguez, S. P. Schwendeman and M. R. Prausnitz, *J. Controlled Release*, 2019, **5**, 8145.
100 Y. Lee, W. Li, J. Tang, S. P. Schwendeman and M. R. Prausnitz, *J. Controlled Release*, 2021, **337**, 676–685.
101 B. Wang, S. Zhang, X. Zhao, J. Lian and Y. Gao, *Drug Delivery Transl. Res.*, 2022, **12**, 944–956.
102 A. Than, K. Liang, S. Xu, L. Sun, H. Duan, F. Xi, C. Xu and P. Chen, *Small Methods*, 2017, **1**, 1700269.
103 A. T. Ehrlich, B. L. Kieffer and E. Darcq, *Expert Opin. Ther. Targets*, 2019, **23**, 315–326.
104 N. Peyravian, E. Dikici, S. Deo, M. Toborek and S. Daunert, *Prog. Neurobiol.*, 2019, **182**, 101679.
105 M. Kovaliov, S. Li, E. Korkmaz, D. Cohen-Karni, N. Tomycz, O. B. Ozdoganlar and S. Averick, *RSC Adv.*, 2017, **7**, 47904–47912.
106 M. Sardesai and P. Shende, *Curr. Drug Delivery*, 2020, **17**, 776–786.
107 M. S. Baig, A. Kolasa-Wołosiuk, A. Pilutin, K. Safranow, I. Baranowska-Bosiacka, J. Kabat-Koperska and B. Wiszniewska, *Int. J. Environ. Res. Public Health*, 2019, **16**, 1726.
108 A. J. Paredes, F. Volpe-Zanutto, A. D. Permana, A. J. Murphy, C. J. Picco, L. K. Vora, J. A. Coulter and R. F. Donnelly, *Int. J. Pharm.*, 2021, **606**, 120885.
109 K. Lee, Y. Xue, J. Lee, H.-J. Kim, Y. Liu, P. Tebon, E. Sarikhani, W. Sun, S. Zhang, R. Haghniaz, B. Çelebi-Saltik, X. Zhou, S. Ostrovidov, S. Ahadian, N. Ashammakhi, M. R. Dokmeci and A. Khademhosseini, *Adv. Funct. Mater.*, 2020, **30**, 2000086.
110 A. Ullah, C. M. Kim and G. M. Kim, *R. Soc. Open Sci.*, 2018, **5**, 171609.
111 G. M. Ullah, A. Kim and C. M. Kim, *R. Soc. Open Sci.*, 2020, 348–349.
112 L. P. Herrera Estrada and J. A. Champion, *Biomater. Sci.*, 2015, **3**, 787–799.
113 S. C. Park, M. J. Kim, S.-K. Baek, J.-H. Park and S.-O. Choi, *Polymers*, 2019, **11**, 369.
114 M. Battisti, R. Vecchione, C. Casale, F. A. Pennacchio, V. Lettera, R. Jamaledin, M. Profeta, C. Di Natale, G. Imparato, F. Urciuolo and P. A. Netti, *Front. Bioeng. Biotechnol.*, 2019, **7**, 296.
115 C. Di Natale, D. De Rosa, M. Profeta, R. Jamaledin, A. Attanasio, E. Lagreca, P. L. Scognamiglio, P. A. Netti and R. Vecchione, *J. Mater. Chem. B*, 2021, **9**, 392–403.
116 A. Panda, A. Shettar, P. K. Sharma, M. A. Repka and S. N. Murthy, *Int. J. Pharm.*, 2021, **593**, 120104.
117 U. Angkawinitwong, A. J. Courtenay, A. M. Rodgers, E. Larrañeta, H. O. McCarthy, S. Brocchini, R. F. Donnelly and G. R. Williams, *ACS Appl. Mater. Interfaces*, 2020, **12**, 12478–12488.
118 Y. Wu, L. K. Vora, Y. Wang, M. F. Adrianto, I. A. Tekko, D. Waite, R. F. Donnelly and R. R. S. Thakur, *Eur. J. Pharm. Biopharm.*, 2021, **165**, 306–318.
119 H.-G. Kim, D. L. Gater and Y.-C. Kim, *Drug Delivery Transl. Res.*, 2018, **8**, 281–290.
120 R. P. Heaney, R. L. Horst, D. M. Cullen and L. A. G. Armas, *J. Am. Coll. Nutr.*, 2009, **28**, 252–256.
121 S. Bhattaccharjee, M. Beck-Broichsitter and A. K. Banga, *Pharmaceutics*, 2020, **12**, 472.
122 K. M. Saifullah and Z. Faraji Rad, *Adv. Mater. Interfaces*, 2023, **10**, 2201763.
123 Z. Faraji Rad, *Adv. Eng. Mater.*, 2023, **25**, 2201194.
124 V. Ebrahiminejad and Z. Faraji Rad, *Adv. Mater. Interfaces*, 2022, **9**, 2201115.